
Università degli Studi di Napoli Federico II

Facoltà di Ingegneria



Francesca Linda Perelli

SEISMIC RESPONSE OF NTS MASONRY BUILDINGS
THROUGH LIMIT STATE AND D. E. M. ANALYSES

Tesi di Dottorato

XXXII Ciclo

TUTOR

Prof. Arch Giulio Zuccaro

CO-TUTORS

Ing. Daniela De Gregorio

Ing. Andrea Montanino

aprile 2020

dottorato di ricerca in ingegneria strutturale, geotecnica e rischio sismico

Contents

Introduction	22
1 The masonry structure	23
1.1 Introduction	23
1.2 Mechanical characteristics of the elements of a masonry wall	24
1.3 The box effect	26
1.4 Mechanical models for masonry behaviour	27
1.5 The masonry distribution on Italian territory	34
2 The seismic vulnerability	43
2.1 Seismic vulnerability assessment approaches	43
2.1.1 Observational approach	44
2.1.2 Mechanical-analytical approach	45
2.1.3 The hybrid approach	47
2.2 Criteria for the definition of the levels of damage	47
2.3 Criteria for the definition of the vulnerability class assignment	48
2.3.1 The E.M.S. 98 Criteria	48
2.3.2 The S.A.V.E. method	50
2.4 Seismic vulnerability assessment tools	55

2.4.1	The Damage Probability Matrices	55
2.4.2	The Vulnerability curves	61
2.4.3	Capacity spectrum method	63
2.4.4	Collapse mechanisms	64
3	Empirical calibration of the vulnerability curves for Italian masonry buildings	65
3.1	Introduction	65
3.2	Calibration	66
3.2.1	Harmonization of the database	68
3.2.2	Mathematical calibration of the vulnerability curves	71
3.3	L'Aquila 2009: a validation of the outcomes calculated through the IRMA platform	84
4	Seismic behaviour of masonry buildings, out of plane and in plane, through limit state and D.E.M. analyses	91
4.1	Introduction	91
4.2	Model of the out of plane behaviour - Limit analysis	94
4.2.1	Simple overturning	97
4.2.2	Vertical bending	98
4.2.3	Horizontal bending	103
4.3	Model of the in plane behaviour - D.E.M. analysis	103
4.3.1	The wall discretization	106
4.3.2	The static values in the contact points . . .	110
4.3.3	The stiffness matrix	116
4.3.4	The mass matrix	121
4.3.5	The damping matrix	121
4.3.6	The Newmark method	122
4.3.7	The time step	124
4.3.8	The achievement of the levels of damage .	125

4.4	The vulnerability factors	126
5	Simulations and outcomes	133
	Conclusions	151

List of Figures

1.1	Monoaxial tests on prisms of masonry	25
1.2	Completeness of survey activities in CARTIS in reference to the number of buildings	35
1.3	Completeness of survey activities in CARTIS in reference to the population	36
1.4	Completeness of survey activities in CARTIS in reference to the municipalities	36
1.5	Masonry typologies distribution on Italian regions .	37
1.6	Correlation between the kind of masonry and demo- graphic classes	38
2.1	Grade of damages according to the EMS98	49
2.2	Vulnerability classes depending on the vertical struc- tures according to the EMS'98	51
2.3	Example of influence of the horizontal structure in the vulnerability behaviour	54
2.4	Buildings parameters considered by Whitman 1973	56
2.5	Levels of damage defined by Whitman 1973	57
2.6	Example of damage probability matrix produced by Whitman 1973	58

List of Figures

2.7	Damage probability matrices produced by Zuccaro et al. 2000	60
2.8	Example of vulnerability curve (Polese, 2002) . . .	62
3.1	The adopted empirical procedure	67
3.2	Vulnerability curves for Italian masonry buildings in class A - without assumptions	75
3.3	Vulnerability curves for Italian masonry buildings in class B - without assumptions	76
3.4	Vulnerability curves for Italian masonry buildings in class C - without assumptions	77
3.5	L'Aquila shakemap	79
3.6	Vulnerability curves for Italian masonry buildings in class A - with assumptions	81
3.7	Vulnerability curves for Italian masonry buildings in class B - with assumptions	82
3.8	Vulnerability curves for Italian masonry buildings in class C - with assumptions	83
3.9	buildings distribution on the levels of damage in reference to the whole area and the effective AE-DES forms	85
3.10	buildings distribution on the levels of damage in reference to the whole area and the integrated AE-DES forms	86
3.11	buildings distribution on the levels of damage in reference to the municipalities fully detected	86
3.12	buildings distribution on the levels of damage in reference to the municipalities with $p_{ga} < 0.05g$. .	87
3.13	buildings distribution on the levels of damage in reference to the municipalities with $p_{ga} > 0.20g$. .	87

3.14	number of buildings on the levels of damage in reference to the whole area	88
4.1	Global mechanisms of collapse for the masonry buildings according to Medea	93
4.2	Simple overturning of one floor in a buildings with more floors	97
4.3	Simple overturning of the wall	98
4.4	Simple overturning - a section view	99
4.5	Vertical bending for a building of two floors	100
4.6	Vertical bending for one floor	100
4.7	Vertical bending for one floor, a section view . . .	101
4.8	Vertical bending for two floors, a section view . . .	102
4.9	Horizontal bending phenomena	104
4.10	Horizontal bending, a section view	104
4.11	The elements constituting the wall	107
4.12	The modelling of the wall: the control points . . .	108
4.13	The contact areas associated to the control points .	108
4.14	Reference Systems associated to the control points of an element	109
4.15	Verifying of connection among the control points .	110
4.16	Displacements in the local system	112
4.17	Cycle to define the mechanical field of the mortar in the control points	117
4.18	Example of the composition of the stiffness matrix	118
4.19	Example of the composition of the submatrix of the element 1	119
4.20	Example of the composition of the stiffness matrix	120
4.21	Vulnerability factor: number of floors	128
4.22	Vulnerability factor: horizontal structure	128
4.23	Vulnerability factor: horizontal connections	129

4.24	Vulnerability factor: openings	129
5.1	Vulnerability curve D2 for the in plane analysis in reference to the considered sample	136
5.2	Vulnerability curve D3 for the in plane analysis in reference to the considered sample	137
5.3	Vulnerability curve D4 for the in plane analysis in reference to the considered sample	137
5.4	Vulnerability curve of simple overturning in refer- ence to the considered sample	138
5.5	Vulnerability curve of vertical bending in reference to the considered sample	138
5.6	Vulnerability curve of horizontal bending in refer- ence to the considered sample	139
5.7	Vulnerability curves of in plane and out of plane phenomena	140
5.8	Vulnerability curve D3 for the in plane analysis with reference to the influence of the number of floors	141
5.9	Vulnerability curve D4 for the in plane analysis with reference to the influence of the number of floors	142
5.10	Vulnerability curve of simple overturning with ref- erence to the influence of the number of floors . . .	142
5.11	Vulnerability curve of vertical bending with refer- ence to the influence of the number of floors	143
5.12	Vulnerability curve D3 for the in plane analysis with reference to the influence of the ties	143
5.13	Vulnerability curve D4 for the in plane analysis with reference to the influence of the ties	144

5.14	Vulnerability curve of simple overturning with reference to the influence of the ties	144
5.15	Vulnerability curve of vertical bending with reference to the influence of the ties	145
5.16	Vulnerability curve of vertical bending with reference to the influence of the ties	146
5.17	Vulnerability curve of vertical bending with reference to the influence of the ties	147
5.18	Vulnerability curve of vertical bending with reference to the influence of the ties	147

List of Tables

1.1	Density and comprehensive resistance of the natural stones (Curioni 1868)	39
1.2	Traction resistance of the natural stones (Curioni 1868)	40
1.3	Density and comprehensive resistance of the bricks (Curioni 1868)	40
1.4	Traction resistance of the bricks (Curioni 1868)	40
1.5	Density and comprehensive resistance of the binding materials (Curioni 1868)	41
1.6	Traction resistance of the binding materials (Curioni 1868)	41
1.7	Mechanical characteristics of the masonries MU6H (Binda et al.1994)	41
1.8	Characteristic resistance to compression of masonry with bricks according to the DM.20.11.1987	42
1.9	Characteristic resistance to compression of masonry with natural stone according to the DM.20.11.1987	42
2.1	Ranges of SPDv for each vulnerability class	53
2.2	Damage probability matrices for vulnerability class A produced by Braga et al (1982)	59

2.3	Damage probability matrices for vulnerability class B produced by Braga et al (1982)	59
2.4	Damage probability matrices for vulnerability class C produced by Braga et al (1982)	61
3.1	Conversion from damage reported in Irpinia Form and EMS98 damage	70
3.2	Conversion from damage reported in Abruzzo Form and EMS98 damage	70
3.3	Conversion from damage reported in AeDES Form and EMS98 damage	71
3.4	Damage Probability Matrix of the masonry buildings for the vulnerability class A	72
3.5	Damage Probability Matrix of the masonry buildings for the vulnerability class B	73
3.6	Damage Probability Matrix of the masonry buildings for the vulnerability class C	73
3.7	Error measurement of the vulnerability curve of the class A (without revisions) in reference to the observed data	74
3.8	Error measurement of the vulnerability curve of the class B (without revisions) in reference to the observed data	76
3.9	Error measurement of the vulnerability curve of the class C (without revisions) in reference to the observed data	77
3.10	Error measurement of the vulnerability curve of the class A (with revisions) in reference to the observed data	82

3.11	Error measurement of the vulnerability curve of the class B (with revisions) in reference to the observed data	83
3.12	Error measurement of the vulnerability curve of the class C (with revisions) in reference to the observed data	84
4.1	Stiffness values in elastic and frictional fields for the control points	116
5.1	PGA values for the achievement of the in plane levels of damage for each building of the sample . .	134
5.2	PGA values for the achievement of the out of plane mechanism for each building of the sample	135

Introduction

After the seismic event in Friuli in 1976 and, much more, after the Irpinia event in 1980, the attention to the seismic problem has grown in Italy since the relevant social and economic impact, the number of victims and building structures lost. Italian authorities developed the consciousness of the high seismicity of the peninsula and of the weakness of the Italian built stock to face threats. The awareness of such a kind risks led to the establishment of the National Department of Civil Protection in 1992, a new Institution with the task of managing emergencies due to disastrous events. Starting from this year, an increasing attention has been paid to the prevention and mitigation measures and to the emergency management.

The first step to provide a Civil Protection Plan to respond the needs generated by a seismic emergency is the risk assessment of the exposed assets. Seismic risk is defined as the cumulative assessment, related to the potential total damage generated by the all possible events that can occur in a considered area in a fixed time period. On the other hand, seismic scenario is defined as the probabilistic distribution of the damage, in a given geographical area, caused by a single seismic event with a fixed value (chosen as “reference scenario”), with assigned probability of occurrence. Risk is, therefore, given by the combination of scenarios. In both analyses three

aleatory variables (hazard, exposure and vulnerability) have to be considered according to the convolutions 1 and 2.

$$Risk = Hazard \times Exposure \times Vulnerability \quad (1)$$

$$Scenario = [Single Hazard] \times Exposure \times Vulnerability \quad (2)$$

The “hazard” is the probability of occurrence of a seismic event of a given intensity in a fixed area and in a predetermined time window. The “exposure” is the qualitative and quantitative geographic distribution of the different elements at risk (population, buildings, infrastructures, activities and facilities, etc) which characterize the examined area, whose conditions and/or functionality could be damaged, modified or destroyed since the occurrence of the seismic event. The “vulnerability” is the response of an exposed element at risk to a given seismic, event and it can be assessed as the probability that an exposed element at risk reaches a given level of damage, according to an opportune measurement scale, under the effects of a natural event of given intensity. A correct assessment of the three factors is a fundamental prerequisite to define the risk.

The work presented in this thesis has been developed in the frame of the activities of the PLINIVS Study Centre (<http://plinivs.it/en-home/>), a structure of L.U.P.T. Research Interdepartmental Centre (University of Naples Federico II). The Centre works since 30 years in the development of several probabilistic simulation models to assess the impacts of natural hazards, taking into account the impact distribution in time and space and the cumulative effects given by possible cascading events, as well as a continuous data collection activity on built environment and population, at national and regional scale. Furthermore, since 2006 it is a National Competence Centre on Volcanic Risk for the Italian Civil Protection. The activities of the thesis has been also involved in the framework of tech-

nical board promoted by the Italian Civil Protection with the aim to develop a seismic vulnerability tool for Italian buildings differently classified in function of vertical structures (masonry and reinforced concrete) to assess scenario and risk analyses by IRMA platform, Italian Risk Map [1].

In the framework of these activities, the topic of research presented in this thesis is born. The aim of this research is to furnish a tool able to define vulnerability curves that describe the behaviour of the Italian masonry buildings.

This work proposes two methodologies to assess the vulnerability of the Italian masonry buildings in respect to the seismic actions: the first one is empirical/observational and the second one is analytic. Through the observational method, the behaviour of the masonry buildings has been, determined on the basis of statistical correlations among the most common and influencing typological characteristics of the Italian masonry constructions and the damages that the buildings has suffered as a result of a seismic event. To this purpose, the PLINIVS database, containing information on about 240,000 masonry buildings collected after the main italian seismic events, has been used and correlated to the seismic input values furnished by the INGV, the Italian National Institute of Geology and Vulcanology (<http://www.ingv.it/it/>). This observational evaluation of the vulnerability has the advantage to quickly furnish a final product of the all-inclusive of a fair variety of buildings typologies, although it has the weakness that the outcomes are particularly influenced by the typological distribution of the buildings reported in the considered sample.

The second part of the work provides an analytic tool that define the behaviour of the in plane and out of plane walls of the masonry buildings. These analysis has been focused on buildings with a good connections among perpendicular walls, i. e. well designed

buildings having a good quality masonry and good technological solutions.

With reference to the out of plane behaviour, some mathematical assumption on the masonry material have been done and an analytical model has been developed with the aim to estimate the lower value of seismic input that activate a collapse kinematism. The analyses only considers a façade of the building and the calculation has been done in 2D. The developed model is based on the Heymann assumption on the material, and the façade is considered as a composition of rigid blocks. At the end, the kinematic theorem of the limit analysis has been used to define the conditions of collapse.

The in plane behaviour of the walls has been analyzed through a discrete element method. The model considers walls with rigid blocks, representative of the good quality briks, disposed regular and connected with deformable mortar. The procedure adopts a dynamic analysis that for each temporal step furnishes displacements, velocities and accelerations values of the blocks and the tensional configuration of their interaction through the mortar. The model, also, considers two kinds of interactions depending on the tensional state of the mortar: in particular, before the crack of the mortar an elastic law describes the interaction, while after the crack a friction law is used. Increasing linearly in time the seismic input value, the configuration of the wall for each time step has been calculated and, on the basis of the percentage of cracks and relative distances between contiguous blocks, the evoluion of the damage has been defined.

This thesis has been organized in five Chapters. The Chapters 1 and 2 constitutes a compilation part and concern the contextualization of the treated arguments: masonry and seismic vulnerability. The Chapters 3 - 4 and 5 concern the three methodologies adopted

for the three degree of depth and their outcomes.

Specifically, Chapter 1 describes the mechanical characteristics of the masonry material, the most common technical solutions adopted for the masonry buildings and their distribution on Italian territory.

Chapter 2 presents an overview of the main approaches and tools used for the seismic vulnerability assessment. In particular: the first part contains a brief description of the statistical-observational method and the analytical-mechanical one, the second part outlines the historical evolution of the criteria used for the damage definition and vulnerability class assignment, and, at the end, the third part presents the main observational and analytical tools adopted since 1970 to today.

Chapter 3, the first one of the experimental part, contains the methodology adopted to calculate the vulnerability curves with the first degree of depth. A description of the used database and its harmonization has been depth, and the mathematical calibration on the data has been presented.

Chapter 4 contains the methodologies adopted for the analytical studies of the in plane and out of plane behaviour of the wall. The first part delines the criteria adopted for the out of plane analysis. It is described the methodology to define the low PGA value able to activate the considered mechanism on the basis of the typological characteristics of the wall. The second part describes the structure of the D.E.M. analysis built in MATLAB to define the in plane behaviour of the wall and the assumption adopted on the mortar.

Chapter 5 presents the simulation and the outcomes in terms of vulnerability curves obtained through the models described in the Chapter 4. Some considerations on the influence of the considered parameters and on the interaction among walls with in plane solicitations and walls with out of plane solicitations are also shown.

Chapter 1

The masonry structure

1.1 Introduction

The masonry is one of the oldest and most widespread kind of construction used in the world. The term "masonry" indicates a set of technological techniques particularly varied, and its behaviour is strictly connected to the nature of the materials and the way they are assembled. The main materials that compose the masonry walls are essentially elements with good resistance connected by binding material. The resistant elements can be done in stone or brick; the first ones have a natural origin, and the second ones are artificial.

The natural stone is the oldest used material. It has uniform and good characteristics and an high resistance to the deterioration. Stones can have different dimensions according to their nature. The artificial bricks have mechanical characteristics that depends on the materials used to create them and to the adopted cooking process. The dimensions of the elements are defined by the necessities.

The binding material is generally a mortar obtained by sand and lime. Its mechanical characteristics depend on the used sand and on its adhesion to the lime.

Although the masonry has an easy structure obtained by the composition of two materials only, its behaviour is difficult to define. It depends on the nature of the materials, on the texture in which they are assembled and on the direction of the sollicitation. To define the behaviour of a masonry wall is necessary to analyze the mechanical characteristics of the elements that compose the wall: stones/bricks and mortar.

1.2 Mechanical characteristics of the elements of a masonry wall

The first significant information on the resistance of the masonry elements can be found in treatment *Istruzioni di Architettura, Statica e Idraulica* written by Cavalieri in 1845 [2]. About the bricks, the author report the resistance values produced by previous researches, and also states that if it is not possible testing the bricks to be used it is necessary to adopt the low value reported in his treatment. The range of resistance values indicated by the author is $40 - 170 \text{ kg/cm}^2$. About the stones, the author states that this materials always can be considered with an high resistance ($600 - 1,400 \text{ kg/cm}^2$). In 1876 Gabba produced the first studies on the mortar [3], for which a range of resistance of $6 - 10 \text{ kg/cm}^2$ has been detected.

All these studies have been collected and re-organized in six volumes by Curioni from the 1864 to the 1884 [4]. that in his works summarized the density and the resistance of these materials. In the Tables 1.1 and 1.6 the values of density and resistences for some

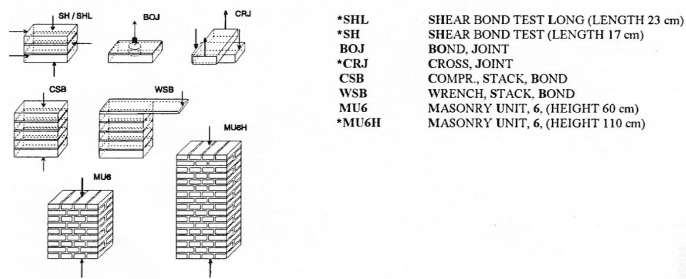


Figure 1.1: Monoaxial tests on prisms of masonry

natural stones, bricks and binding materials have been reported.

At the beginning of the XX century the first studies on the composite material brick-mortar or stone-mortar have been done. In the work produced by Campanella in 1928 [5]) it is shown that the strength of the masonry is bonded by the strength of the mortar if this last is weak in respect to the bricks and, on the other hand, if the quality of the mortar is good the crack is caused by the disintegration of the brick.

Some other important experimental analyses have been produced by Binda in 1994 [6] that studied the behaviour of some masonry prisms having different dimensions and textures. In Figure 1.1 the considered sample have been reported, and in Table 1.7 the corresponding outcomes have been summarized. The author obtained that the behaviour of the masonry is always worse of the bricks and better of the mortar. The experimental campaigns on the masonry structures has been used to define reference legislations useful for designers and researchers. In Italy, for example, the D.M. 20.11.1987 provides the admissible tensions for the masonry structures as reported in the Tables 1.8 and 1.9.

1.3 The box effect

The behaviour of a masonry wall is highly depending on the quality of the material and on their composition, however the response of the global buildings is conditioned by several structural parts that defines its whole resistance in respect to the seismic actions. The behaviour of a building under seismic actions is influenced, in particular, by the technological solutions adopted for the realization of the floors and the grade of connection among the walls. Synthetically, it can be assert that if a building reaches a "box system", i.e. an efficient connection among its parts, its response to the actions is global and, consequently, better.

To understand this phenomena it's enough to examine a paper box: each sheet taken singularly offers a poor resistance to the stress. However, if two orthogonal sheets are connected, a considerable increasing of resistance is obtained. Furthermore, adding a cover (horizontal structure) on the connected sheets, the global resistance considerably increases. For these reasons, the vertical walls and the horizontal floors are the responsables of the resistance.

The floors are the first elements of the structure that distribute the seismic actions on the walls. To well exploit this function they have to be rigids and well connected to the walls. Rigid elements can be obtained if realized in concrete or vaults, however often in the past they have been built in wood that is not able to guarantee the hoped loads distribution. To overcome this problems, some historical buildings have been reinforced by the introduction of "floor curbs", elements realized in reinforced concrete disposed on the perimeter of the wall.

Another solution often adopted with the aim to improve the connection is the introduction of the ties, steel elements disposed in the floors able to connect parallel walls.

1.4 Mechanical models for masonry behaviour

There are two different scale approaches to study the structural response of masonry elements: micro-mechanical model and macro-mechanical model. In the micro-mechanical model, the masonry is considered as a heterogeneous material, represented as an assemblage of mortar and rigid particles of stone or bricks joined held together by compressive forces. The cracks occurring in masonry are usually located at the mortar joint-brick interfaces, which represent planes of weakness due to the coupling of two different materials. The macro-mechanical model is based on the use of phenomenological constitutive laws for the masonry material, considered as a homogenized medium. The very small size of the stones compared to the dimension of the whole structure allows us to consider continuous body instead of a discrete system composed of a large number of particles. The masonry is considered as a continuous body instead of a discrete system composed of a large number of particles [7].

The micro-mechanical model

The most common way to study the micro-mechanical behaviour of the masonry is through the Discrete Element Method (DEM), that was introduced by Cundall 1971 [8] for the analyses of the rock mechanisms and it was subsequently applied to similar problems as modelling the masonry brick elements. The formulation and solution of the method is based on the formulation and the solution of equations of the motion of rigid or deformable bodies. The treatment can be done using an explicit or an implicit approach: in the first case a finite volume method (FVM) is used for the discret-

ization of the system, instead in the second one the discussion uses a finite element method (FEM) to the same purpose.

The DEM provides to study the analysed system as an assemblage of blocks (rigid or deformable) connected in specific points with analytical relations. The motion process provides to update in each considered time step the deformation and the tensile status of the system. The DEM is not a continuum method since the contact patterns between the components continuously change. The structure of a DEM analysis is articulated in three macro-step: identification of block system configuration, evaluation of the solution of equations of motion of the block system for each time step, updating of varying contacts between the blocks. Analyses of system constituted by rigid blocks are often treated with an explicit time-marking that allows to easily calculate the solution of the dynamic equation of the motion.

The most representative explicit DEM methods is the Distinct Element Method created by Cundall [9], [10]. Other developments have been made in parallel with the distinct element approach and used the name ‘discrete element methods’, such as in [11], [12] and [13].

Explicit DEM -

The first formulation of the explicit DEM was proposed in [14] with the aim to define the structure of a discrete element program. In particular indications for the representation of contacts, the representation of solid material; and for the scheme used to detect and revise the set of contacts are reported.

The explicit discrete element method is based on a discretization of the system according to an FVM scheme that represents the individual blocks composing the domain as polygons subdivided into a finite number of triangles (2D analysis) or tetrahedra (3D ana-

lysis) An explicit Lagrangian formulation is used to represent the deformations of the blocks, while the kinematic condition of the contacts is described on the basis of the smallest distance between two contiguous blocks, pre-set in the model. In particular, when this distance is within a prescribed threshold, a potential contact between these two blocks is numerically established. The contact-law is also depending on the gap between the blocks. In particular, interaction between two contacting blocks is described by a force related to a stiffness value, depending in the material of the contact, in the normal direction and a force depending on a stiffness or a friction value in the tangential directions, with respect to the contact statement.

To be more exhaustive, the interaction is described by a stiffness model that provides a relationship between the contact force and its displacement like in the Equations 1.1 and 1.2.

$$F_n = k_n \cdot U_n \quad (1.1)$$

$$F_t = k_t \cdot U_t \quad (1.2)$$

in which F_n is the contact force in the normal direction, F_t is the contact force in the tangential direction, k_n is the stiffness in the normal direction, k_t is the stiffness in the tangential direction, U_n is the normal displacement in the direction between the two blocks and U_t is the tangential displacement in the direction between the two blocks. When the tangential force matches the maximum admissible value of the tangential contact force, the tangential contact response has an attritive nature. So, the frictional contact is modelled as like in the Equation ??

$$F_t^i \geq_i^{max} = \mu \cdot |F_n^i| \quad (1.3)$$

in which F_t^i is the tangential force in the generic point i , F_i^{max} matches the maximum admissible value of the tangential contact

force in the generic point i , μ is the minimum frictional coefficient among the contact bodies and F_n^i is the normal force in the generic point i . At the end, the contact model in the normal direction can be modelled as a:

- soft contact model, if the value of the contact force in the normal direction is zero in the initial instant and depending on the displacements (positive and negative) in the others step time. This model can be used in case of low values of tension and friction;
- hard contact model, if the compenetrating between the block is allowed. Mathematically, the concept of contact ‘overlap’ can be accepted since the deformability description. This model is suggested in case of high values of tension and friction.

From a numerical point of view, the solution is described by an algorithm that proceeds by successive steps and describes the dynamic behaviour of the system; during time steps the acceleration is generally assumed to be constant or linear. In the formulation it is necessary to use sufficient small time-steps such that the perturbations within the system can only propagate from one element to the contiguous ones. At any time, the resulting forces on any element are, therefore, determined exclusively by its interaction with those to which it is in contact. The algorithm used to integrate the equation of motion is an explicit central difference scheme as opposed to the implicit approach utilized in other continuum based on numerical methods. The contact and inertial forces of the block are determined locally at each time step from the known variables on the boundaries. In particular, the second Newton law for a generic

block i can be written as in the Equations 1.4 and 1.5.

$$v_i t + \Delta t/2 + [\frac{\sum f_i}{m} + b_i]\Delta t \quad (1.4)$$

$$\omega_i^{t+\Delta t/2} = \omega_i^{t-\Delta t/2} + \frac{\sum M_i}{I} \Delta t \quad (1.5)$$

where v_i and ω_i are the translational and rotational velocity respectively, Δt is the time step, m is the mass of the block, I is the moment of inertia, b_i is the vector of the volume force component in the blocks, M_i is the vector of the resultant moments. The displacements in the next time step can be evaluated as in the Equations 1.6 and ??

$$u_i^{t+\Delta t} = u_i^t + v_i^{t+\Delta t/2} \Delta t \quad (1.6)$$

$$\theta_i^{t+\Delta t} = \theta_i^t + \omega_i^{t+\Delta t/2} \Delta t \quad (1.7)$$

in which u_i and θ_i are the translational and angular displacement components.

Implicit DEM - Distontinuous Deformation Analysis method

The DDA method was proposed the first time in which a back analysis algorithm is proposed with the aim to define the best approximation of the deformed configuration of the block system starting from known displacements and deformations. The proposed formulation represents the motion and deformation of a regular shaped block depending on three rigid body motion and three constant strain components.

The analysis sinks the roots in the second law of thermodynamic, that says that a loaded system by internal or external forces moves in such a way as to produce the least amount of total energy E , that is given by the sum of the potential energy U , the kinematic energy

K and the dissipate energy W according to the Equation 1.8.

$$E = U + K - W \quad (1.8)$$

Minimizing the equation with respect to the displacements d , the motion equation on the corresponding block can be written as in the 1.9.

$$\frac{\delta E}{\delta d} = \frac{\delta U + \delta K - \delta W}{\delta d} = 0 \quad (1.9)$$

Using this criterium for each element of the dominium, the same system of algebraic equation of the FEM analysis is obtained. In fact, considering a dominium with N blocks, in which each one is discretized in m nodes, having u and v represent normal and tangential displacement of each node, the minimization of the total energy can be written in a matrixial form as in the Equation 1.10

$$\mathbf{K} \cdot \mathbf{d} = \mathbf{F} \quad (1.10)$$

The macro-mechanical model

One of the most common method to model the macro-mechanical behaviour of the masonry is through the theory of no tension material, originally formulated by Heyman [15], [16]. In these treatments the masonry is modelled like an assemblage of rigid elements that can react to compressive forces only but are incapable of sustaining any tensile stress. In literature several studies about bodies with no tension behaviour of elastic been done by many authors [17],[18],[19],[20] and [21]. Even if this approach is based on very strong simplifications and the representation of the behaviour of the masonry is not particularized, it is efficient as tool for the structural assessment of the safety of buildings. In order to define the model no-tension material, it is useful to recall the assumptions introduced by Heyman:

-
- Stone has no tension strength: The model does not consider the capacity of the material to resist to tension strength. Allowed deformation are inelastic only, and the collapse mechanisms are always characterized starting from the opening of cracks in tension zones and after by the activation of the kinematism. No tensile forces can be transmitted from one portion of the structure to another.
 - Stone has an infinite compressive strength: Even if the assumption is unsafe, the errors introduced are very small since this hypothesis can be considered adequate if the collapse is accompanied by low compressive stresses, only.
 - Sliding failure cannot occur: The assumption considers that that friction is high enough, or that the stone are effectively interlocked, so that the elements cannot slide on each other. It implies that wherever there is a weak plane, for example between the bricks, the line of thrust should not depart too far from normality in the plan.

The above no-tension conditions for the masonry continuum can be formulated in a more general form in the Equation 1.11, so that of the body, the maximum eigenvalue of the normal stress tensor σ_{max} cannot be positive because the stone has zero tensile strength and the 3x3 matrix $\sigma_{ij}(i, j = x, y, z)(i, j = x, y, z)$ results in being negative semi-definite. In terms of stress components in the plane case the no-tension condition can be restated as in the Equation 1.12

$$\sigma_{max} \leq 0 \quad (1.11)$$

$$\phi = \sigma_{max} = \frac{\sigma_x + \sigma_y}{2} + \sqrt{\frac{(\sigma_x - \sigma_y)^2}{4} + \tau_{xy}^2} \leq 0 \quad (1.12)$$

$$\psi = \epsilon_{min}^c = \frac{\epsilon_x^c + \epsilon_y^c}{2} - \sqrt{\frac{(\epsilon_x^c - \epsilon_y^c)^2}{4} + \epsilon_{xy}^{c2}} \geq 0 \quad (1.13)$$

$$\sigma_{ij}\epsilon_{ij} = 0 \quad (1.14)$$

1.5 The masonry distribution on Italian territory

A big part of Italian Masonry buildings have been constructed in very ancient times, and not always with good quality materials or techniques. Often, the choice of the material has been conditioned more by the local availabilities than by a good previous design. For these reasons, Italian territory is reach of a particularly widespread of masonries that often have a not good behaviour. The knowledge of the quantities and the distributions of the masonry types on Italian soil is one of the useful instruments for the analysis of risk.

In a work developed for the line of research CARTIS, a study of the masonry buildings distribution on Italian territory has been done. In particular, some teams of technician have detected, among a lot of information, the prevalent masonry structure of each buildings compartment present in the studied areas. In Figures 1.2, 1.3 and 1.4 have been resumed the completeness of the survey of buildings for each Italian region, expressed as a function of the total number of buildings, population and municipalities within the region.

In particular, it is shown that the best completeness value can be founded in Campania about number of buildings and population, and in Basilicata about the number of municipalities. In Figure 1.5 is represented the distribution of the masonry typologies for each Italian region. It is shown that a quantity mayor of the 50% of

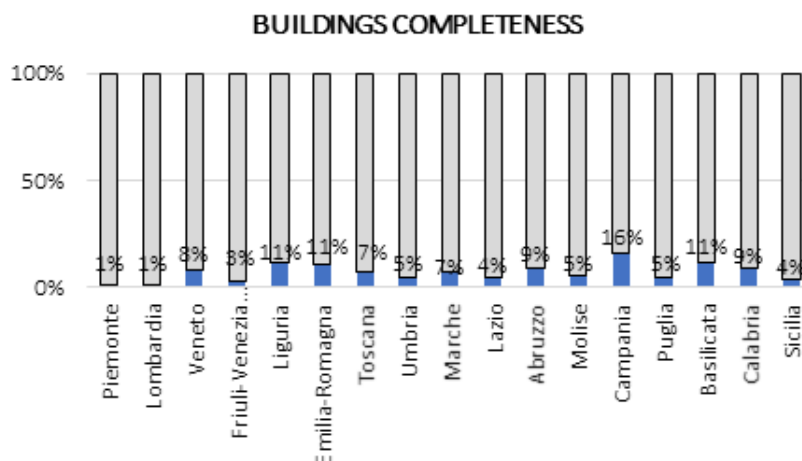


Figure 1.2: Completeness of survey activities in CARTIS in reference to the number of buildings

poor-quality masonry can be founded the regions of Calabria, Molise, Toscana and Lombardia, instead a quantity mayor of the 50% of good masonry is in Sicilia, Campania, Abruzzo, Marche, Umbria, Emilia Romagna, Friuli Venezia Giulia, Veneto and Piemonte. Moderate quantities of slab-shaped or almost regular masonry is in Puglia, Molise and Liguria. Another interesting result is also shown in Figure 1.6 in which the correlation between the kind of masonry and the demographic classes of the municipalities is shown. In particular, it can be noticed that quality of the masonry increases if the demographic class increase.

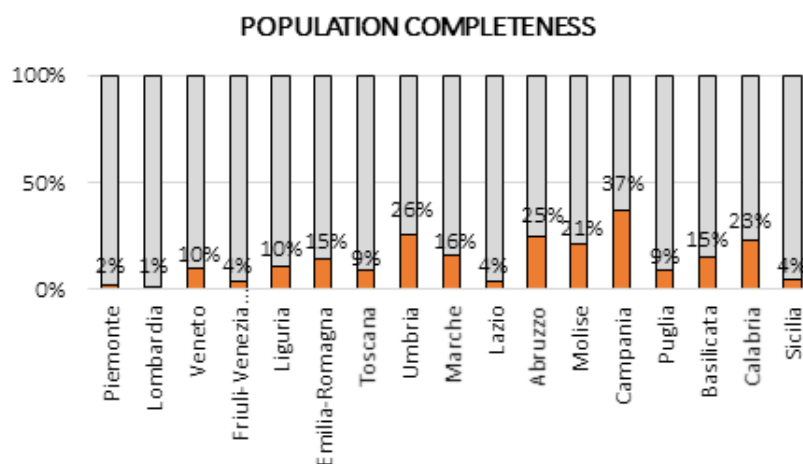


Figure 1.3: Completeness of survey activities in CARTIS in reference to the population

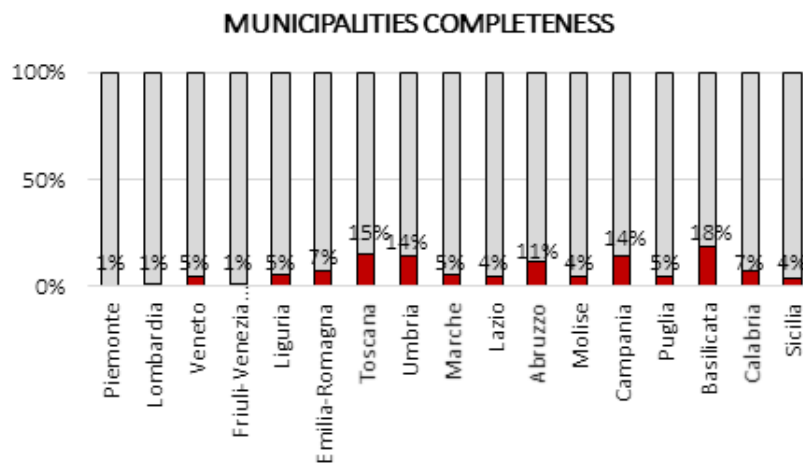


Figure 1.4: Completeness of survey activities in CARTIS in reference to the municipalities

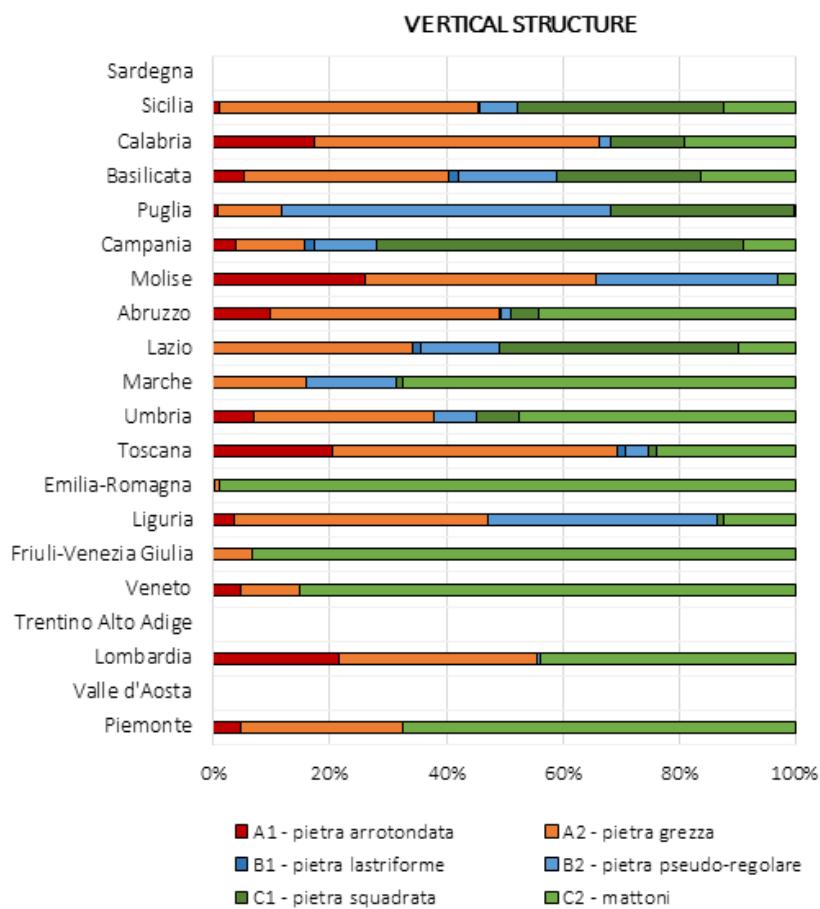


Figure 1.5: Masonry typologies distribution on Italian regions

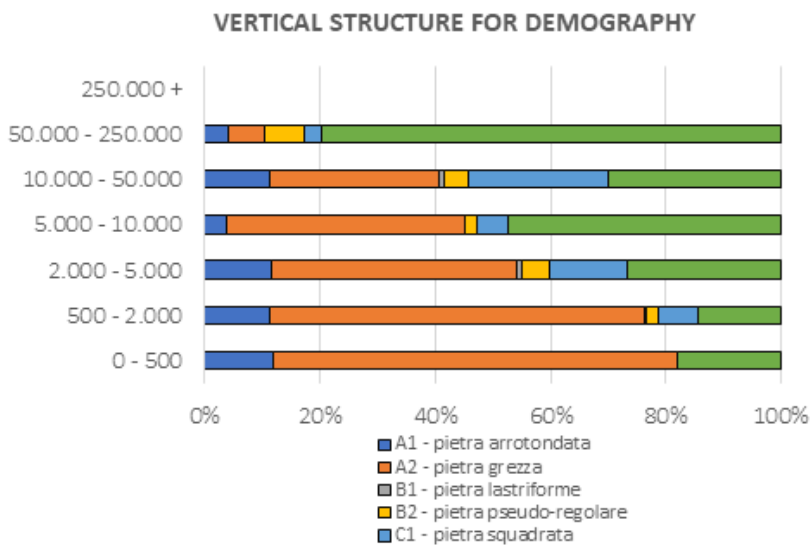


Figure 1.6: Correlation between the kind of masonry and demographic classes

Table 1.1: Density and compressive resistance of the natural stones (Curioni 1868)

PIETRE NATURALI	Densità [kg/dm ³]	Resistenza a compressione [kg/cm ²]
Calcari teneri	1.40 - 2.20	60 - 130
Calcari mezzani	2.20 - 2.60	130 - 200
Calcari duri	2.60 - 2.90	300 - 500
Marmo di candoglia sul Lago Maggiore	2.70	300
Marmo bianco di Carrara	2.71	320
Marmo nero di Varenna sul Lago Maggiore	2.72	340
Marmo di Genova	2.70	360
Marmo turchino di Genova	2.71	600
Marmo bianco venato presso Carrara	2.72	650
Pietre silicee tenere	1.40 - 2.20	4-90
Pietre silicee mezzane	2.20 - 2.60	90 - 420
Pietre silicee dure	2.60 - 2.90	420 - 800
Granito rosso di Baverno	2.60	680
Pietra arenaria di Viganò	2.21	140
Pietra di Viggiù	2.23	150
Pietra argillosa di Firenze	2.56	420
Pietre vulcaniche tenere	0.60 - 2.20	34-230
Pietre vulcaniche mezzane	2.20 - 2.60	230-590
Pietre vulcaniche dure	2.60 - 2.95	590 - 2.000
Pietra pomice	0.60	34
Tufo di Roma	1.22	57
Lava nera di Napoli	1.72	160
Lava grigia di Roma (peperino)	1.97	228
Lava di Napoli (piperno)	2.61	592
Basalti	2.95	2.000

Table 1.2: Traction resistance of the natural stones (Curioni 1868)

PIETRE NATURALI	Resistenza a trazione [kg/cm ²]
Basalto d'Alvernia	77
Calcare di Portland	60
Calcare bianco a grana fina ed omogenea	144
Calcare litografico a tessuto compatto	308
Calcare a tessuto arenaceo	229
Calcare a tessuto dolitico	137

Table 1.3: Density and comprehensive resistance of the bricks (Curioni 1868)

MATTONI	Densità [kg/dm ³]	Resistenza a compressione [kg/cm ²]
Mattoni crudi		33
Mattoni poco cotti	2.09	40
Mattoni cotti a giusto grado	2.17	60
Mattoni il cui grado di cottura supera di poco il punto giusto	2.10	70
Mattoni troppo cotti	1.56	150

Table 1.4: Traction resistance of the bricks (Curioni 1868)

MATTONI	Resistenza a trazione [kg/cm ²]
Mattoni di Provenza, ben cotti	19.5
Mattoni ordinari, deboli	8.0

Table 1.5: Density and compressive resistance of the binding materials (Curioni 1868)

MALTE E CEMENTI	Densità [kg/dm ³]	Resistenza a compressione [kg/cm ²]
Malta comune di calce grassa e sabbia	1.70	19
Malta di calce mediamente idraulica e sabbia	1.70	74
Malta di calce eminentemente idraulica e sabbia	1.70	144
Malta in parti eguali di cemento di Vassy e sabbia 15 gg	1.65	136
Malta di calce grassa e sabbia a 18 mesi	1.63	30
Malta di calce grassa e coccio a 18 mesi	1.46	47
Malta di calce grassa e di pozzolana di Roma o di Napoli a 18 mesi	1.46	37
Gesso impastato con acqua	1.46	50
Gesso impastato con latte di calce	1.57	72
Gesso impastato duro	1.40	90
Calcestruzzo fatto con buona malta idraulica a 18 mesi	2.20	48

Table 1.6: Traction resistance of the binding materials (Curioni 1868)

MALTE E CEMENTI	Resistenza a compressione [kg/cm ²]
Gesso impastato solidamente	120
Gesso impastato con metodo ordinario e un po' di sabbia	4
Malta di calce grassa e di sabbia a 14 anni	3.5
Malta di cattiva qualità di calce grassa e sabbia	0.8
Malta di calce idraulica ordinaria e sabbia a 18 mesi	8
Malta con calce eminentemente idraulica a un anno	14
Malta di parti eguali di cemento Pouilly e sabbia a 1 anno	9.6
Malta di parti eguali di cemento di Vassy e sabbia a 6 mesi (in acqua)	9.6
Malta di parti eguali di cemento di Vassy e sabbia a 1 anno (in acqua)	15.1
Malta di puro cemento di Vassy ad 1 anno (in luogo umido)	20.7
Malta di parti eguali di cemento di Vassy e sabbia ad 1 mese (in acqua di mare)	11.3
Malta di puro cemento di Vassy ad 1 mese	8.5

Table 1.7: Mechanical characteristics of the masonries MU6H (Binda et al.1994)

	f_u [MPa]	ϵ_u [10 ⁻³]	$E_{s(30-50\%)}$ [MPa]	$\epsilon_h/\epsilon_v(AB)$ (30-60%)	$\epsilon_h/\epsilon_v(CD)$ (30-60%)	$\epsilon_h/\epsilon_v(ABCD)$ (30-60%)
MU6H-1	5.75	6.4	1281	-0.26	-0.24	-0.25
MU6H-2	5.66	5.4	2411	-0.14	0.15	-0.14
MU6H-3	6.06	5.81	1255	-0.19	0.10	-0.14
MU6H-4	6.01	6.22	1389	-0.15	-0.21	-0.18
MU6H-5	7.52	5.06	2040	-0.14	-0.14	-0.14
MEDIA	6.20	5.79	1491	-0.18	-0.17	-0.18

Table 1.8: Characteristic resistance to compression of masory with bricks according to the DM.20.11.1987

Resistenza del mattone [MPa]	Classe della malta			
	M1 ($f_k \geq 12MPa$)	M2 ($f_k \geq 8MPa$)	M3 ($f_k \geq 5MPa$)	M4 ($f_k \geq 2.5MPa$)
2.0	1.2	1.2	1.2	1.2
3.0	2.2	2.2	2.2	2.0
5.0	3.5	3.4	3.3	3.0
7.5	5.0	4.5	4.1	3.5
10.0	6.2	5.3	4.7	4.1
15.0	8.2	6.7	6.0	5.1
20.0	9.7	8.0	7.0	6.1
30.0	12.0	10.0	8.6	7.2
40.0	14.3	12.0	10.4	-

Table 1.9: Characteristic resistance to compression of masory with natural stone according to the DM.20.11.1987

Resistenza della pietra [MPa]	Classe della malta			
	M1 ($f_k \geq 12MPa$)	M2 ($f_k \geq 8MPa$)	M3 ($f_k \geq 5MPa$)	M4 ($f_k \geq 2.5MPa$)
2.0	1.2	1.2	1.2	1.2
3.0	2.2	2.2	2.2	2.0
5.0	3.5	3.4	3.3	3.0
7.5	5.0	4.5	4.1	3.5
10.0	6.2	5.3	4.7	4.1
15.0	8.2	6.7	6.0	5.1
20.0	9.7	8.0	7.0	6.1
30.0	12.0	10.0	8.6	7.2
40.0	14.3	12.0	10.4	-

Chapter 2

The seismic vulnerability

2.1 Seismic vulnerability assessment approaches

In the last 30 years some experimental approaches for the vulnerability assessment of the building behaviour have been developed. These methodologies can be grouped in two typologies: the observational-statistical approach and the mechanical analytical approach. Furthermore, recent works are implementing a third method (the hybrid one) that combines the mechanical and observational analyses of the damages produced by past event with the aim to overcome the weaknesses of both approaches.

The choice of the procedure to adopt strictly depends on the available resources and the scale and aim of the study. In fact, the statistical approach can be used for large scale studies to define damage scenarios. However, if the purpose of the study is to identify the seismic behaviour of a single building, or a little group of buildings, with the aim to increase their seismic resilience, a suitable mechanical procedure should be preferred. In the following, a brief description of the two methods is proposed, and a mention to the

third one is reported.

2.1.1 Observational approach

The observational methods exploit a semi-empirical statistical observational approach and are essentially based on the results of the damage detection carried out in the post-earthquake period on a large number of buildings. The statistical correlations are calculated among the reached level of damage, the input hazard and the typological characteristics (vulnerability factors) of the analysed building. Once determined these correlations on the sample of damaged buildings, it is possible to carry out a criteria for merge buildings with similar behaviour in vulnerability classes on the basis of their vulnerability factor, and to describe their behaviour (the corresponding damage to the considered input value) with a mathematical form. The first observational works have been proposed early 70's and the considered input hazard to describe the behaviour of the building was expressed in macro-seismic intensities. Generally, these results of the statistical calibration are reported in Damage Probability Matrices (DPM).

The observational assessment is sufficiently simple, but it is strictly influenced by the engineering sensitivity of the surveyor and by the dimension of the sample and its contents. In fact, a high number of detected buildings doesn't guarantee an efficacious calibration of the correlations if the buildings are similar to each other or if the all the sample is concentrated on the same input hazard value. With the aim to produce reliable statistical analysis, large sets of data are needed to cover the whole range of performances of a given building typology to the whole range of possible seismic hazard considered, and multiple observations of building performance for the same level of input. There are three main types of statistical

tools using in statistical approach for the seismic vulnerability assessment of buildings: damage probability matrices (DPM), Vulnerability Index Method and vulnerability functions. Some important works with observational approach have been produced in [22], [23], [24], [26], [27], [28], [29], [30].

2.1.2 Mechanical-analytical approach

The methods in the second category are based on a mechanical approach, i.e. direct assessment of the seismic capacity of the individual building or groups of buildings. In particular, the response of a building is calculated, representative of a typology, by using structural analysis techniques and numerical tools.

Obviously, the adoptability of this kind of methodologies requires an in-depth knowledge of the construction and a relatively long time to carry out the corresponding assessment. Therefore, apart from the intrinsic difficulties connected to the carrying out of a correct seismic analysis of existing buildings, they are not easily applicable in evaluations on an urban scale both from the technical point of view and from the temporal and economic one.

The reliability of the results depends on the accuracy of the model to reproduce the main characteristics of the buildings and their structural behaviour. It is also dependent on the numerical tools available and by the ability of the researcher to interpret the results. One of the strongness of this method is to frame the problem of seismic vulnerability of masonry structures in structural engineering terms, defining their vulnerability as a direct function of building characteristics.

The required data for these approaches can be extracted from the results coming from the observational approach, that can give information on the significant vulnerability parameters, and from the

sensitivity of the scholar. The required data can also be different on the basis of the adopted methodology. Furthermore, when the aim of the work is to study a specific geographical area the modelled typologies of buildings must be congruent with the typologies in the analysed area. It's important, therefore, to combine the mechanical work for the study of the behaviour of the building, a study of the spread of building types in the territory considered.

According to "Norme Tecniche per le Costruzioni" (DM 14-1-2008) the macro-modelling mechanical methods used to predict the seismic performance of a building are linear static analysis, linear dynamic analysis, nonlinear static analysis and nonlinear dynamic analysis. The last two are considered the most accurate methods for predicting Reinforced Concrete building response to earthquake ground motion. Mechanical methods are based on the application of kinematics models, which identify lateral collapse load multipliers of a given configuration of macro-elements and loads by imposing either energy balance or equilibrium equations. These methods present the advantage of requiring few input parameters to estimate the vulnerability and to identify the occurrence of possible in-plane or out of plane mechanisms for a given building.

Furthermore, the micro-modelling method can be used to analyse the structure. Using these approaches, the masonry wall is discretized in its minimum elements (the bricks/stones) and their interactions are described on their interfaces. These methodologies allow to implement the dynamic behaviour of the analysed wall, and to describe in detail the evolution in the time of the patterns crack and the strain configuration. Although these calculation approach provides a better completeness of the results, it's important to highlight that they need more expensive calculation times.

Some important references can be found in [31], [32], [33], [34], [43], [36], [37], [38], [39], [40], [41] and [42].

2.1.3 The hybrid approach

Hybrid methods combine post-earthquake damage statistics with simulated one, in which analytical damage statistics from a mathematical model of the building typology are carried out. These methods are useful when there is a lack of damage data at certain intensity levels for the geographical area under consideration and they also allow calibration of the analytical methods.

The main difficulty in the use of hybrid methods is that the two vulnerability curves, statistical and mechanical, include different sources of uncertainty and are thus not directly comparable. In the mechanical curves the sources of uncertainty are clearly defined during the generation of the curves whilst the specific sources and levels of variability in the statistical data are not quantifiable. The method used to calibrate the mechanical vulnerability curves using statistical data should include the additional uncertainty present in the statistical data which is not accounted for in the mechanical data. Examples of hybrid approaches can be found in [43] and [44].

2.2 Criteria for the definition of the levels of damage

One of the most shared reference for the definition of levels of damage is found within the EMS 98 guide [45]. This treatment essentially grades the damage in six levels that ideally represent a linear increase in the strength of shaking. The definition of these damages is influenced by the need to describe damage classes which can be readily distinguished by the operator.

The variety of building typologies makes difficult the summariza-

tion of the damages few levels since different types of building respond and fail in different ways to the seismic input. Furthermore, the locations of damages and their patterns may also be different for engineered and non-engineered structures. So, the definition of the damages is distinct in macro-typologies. The first distinctness adopted for definition the level is to recognize the difference between structural and non-structural damage, and carefully distinguish between damage to the primary (load bearing/ structural) system and damage to secondary (non-structural) elements (like infills or curtain walls). The second distinctness, established that the damage is structural, takes into account possible collapse of the structure. So, on the basis of these macro typologies of damage (no structural damage, structural damage and collapse) the six following levels: D0: no damage, D1: Negligible to slight damage; D2: Moderate damage; D3: Substantial to heavy damage; D4: Very heavy damage; D5: Destruction (Figure 2.1).

2.3 Criteria for the definition of the vulnerability class assignment

2.3.1 The E.M.S. 98 Criteria

The EMS'98 also represents one of the most important references for building vulnerability classification, in which a criterium is described. It contains a subdivision that is not generic and allows a sufficiently clear and precise allocation. The discussion distinguishes, first, the buildings according to the structural material: masonry, reinforced concrete, steel, wood, for each category are then identified different types of constructions.

For masonry constructions, seven types are considered which rep-






Classification of damage to masonry buildings	
	Grade 1: Negligible to slight damage (no structural damage, slight non-structural damage) Hair-line cracks in very few walls. Fall of small pieces of plaster only. Fall of loose stones from upper parts of buildings in very few cases.
	Grade 2: Moderate damage (slight structural damage, moderate non-structural damage) Cracks in many walls. Fall of fairly large pieces of plaster. Partial collapse of chimneys.
	Grade 3: Substantial to heavy damage (moderate structural damage, heavy non-structural damage) Large and extensive cracks in most walls. Roof tiles detach. Chimneys fracture at the roof line; failure of individual non-structural elements (partitions, gable walls).
	Grade 4: Very heavy damage (heavy structural damage, very heavy non-structural damage) Serious failure of walls; partial structural failure of roofs and floors.
	Grade 5: Destruction (very heavy structural damage) Total or near total collapse.

Figure 2.1: Grade of damages according to the EMS98

resent rather well the Italian construction tradition, very varied in materials, installation technique and construction details. It is significant to note that priority is given to the quality of the masonry material, which constitutes the seismic-resistant elements of the construction (walls); at this first level of classification it is assumed that the quality of the other elements that influence the response are, on average, consistent with the type of masonry. For example, buildings made of rough stone will generally have worse construction qualities in the floors and connections than those made of rough or split stone; more recent buildings made of masonry not reinforced with artificial elements (bricks, concrete blocks) will in most cases have laterally-concrete horizons.

The scale provides a blurred relationship between the construction types and 6 classes of vulnerability with a decreasing trend from A to F. This relationship is represented by an interval composed of some symbols:

- circle: most of the buildings belong to the class indicated in the
- continuous stroke: indicates a probable interval, i.e. a part of the buildings can belong to that class
- hatching: indicates an interval with very low probabilities, it is about exceptional cases.

2.3.2 The S.A.V.E. method

The definition of the behaviour of a building based on its structural typological characteristics can be also done using the "S.A.V.E." method [46], a procedure for a quick assignment of the seismic vulnerability according to the classification adopted in EMS'98.

Type of Structure		Vulnerability Class					
		A	B	C	D	E	F
MASONRY	rubble stone, fieldstone	○					
	adobe (earth brick)	○	—				
	simple stone	—	○				
	massive stone		—	○	—		
	unreinforced, with manufactured stone units	—	○	—			
	unreinforced, with RC floors		—	○	—		
	reinforced or confined			—	○	—	
REINFORCED CONCRETE (RC)	frame without earthquake-resistant design (ERD)	—	—	○	—		
	frame with moderate level of ERD		—	—	○	—	
	frame with high level of ERD			—	—	○	—
	walls without ERD		—	○	—		
	walls with moderate level of ERD			—	○	—	
	walls with high level of ERD				—	○	—
STEEL	steel structures			—	—	○	—
WOOD	timber structures		—	—	○	—	

○ most likely vulnerability class; — probable range;
 range of less probable, exceptional cases

Figure 2.2: Vulnerability classes depending on the vertical structures according to the EMS'98

The assignment criterion adopted by the EMS98 [45] is essentially based on the characteristics of the vertical structure, with uncertainty intervals in some rather large cases. These uncertainty intervals can also significantly influence risk or impact analyses. "S.A.V.E." method starts from the same concept of the EMS'98 and defines the average behaviour of a building considering its vertical structure. In a second step reduces the uncertainty in the assessment of the vulnerability class through the systematic observation of others typological and structural characteristics of the building influencing the response. These are associated to numerical parameters that represent the vulnerability level modifiers, applied within a rapid vulnerability estimation algorithm. Numerically, the weight of each of these parameters is evaluated through the statistical analysis on the PLINIVS database of typological recurrences and seismic damage recorded during past earthquakes.

The "S.A.V.E". method proposes the definition of vulnerability classes on the basis of the vertical structure behaviour. In particular, three classes of Vertical Structure (VS) are defined as below:

- V0- "Generic" masonry (in the absence of information on the quality of the wall structure)
- V1 - Weak and irregular masonry.
- V2 - Regular and good quality masonry

Each building in the database is assigned the corresponding V_i class. The response of buildings grouped by class is examined for each level of seismic intensity and damage distributions are defined (D0, D1, D5). For each of the three VS damage distributions the Synthetic Damage Parameter (SPD_{V_i}) is estimated, identifying it as the barycentric abscissa of the damage distribution. On the basis of this analysis, three ranges of SPD representative of the VS

Table 2.1: Ranges of SPDv for each vulnerability class

	class A	class B	class C
SPDVmax	5.00	2.20	1.60
SPDVmin	2.20	1.60	0.00

are evaluated (Table 2.1) In particular, Class A represents the weak and irregular masonry, class B the “Generic” masonry and class C1 the regular and good quality masonry.

The modifier that can improve or worsen the average behaviour of a building under seismic action and, consequently, influence the assignment of the vulnerability class are essentially: the horizontal structure, the horizontal connection, the kind of roof, the number of floor, the age, the position of the building in the aggregate. With the aim of evaluating their influence, the SPD_{Vi-Pjk} is estimated on the sample of buildings with a chosen VS and the considered parameter. For example, with the purpose to evaluate the influence of the horizontal structure on “Generic” masonry (V0) buildings, SPD_{V0-Pjk} value is calculated for V0 with wooden floor sample, V0 with steel floor sample, etc. The difference between SPD_{Vi-Pik} value and the SPD_{Vi} value defines the influence of the modifier k of the parameter P_j in the vertical structure V_i . An example of the influence of the parameter is represented in Figure 2.3. At the end, for each building, assumed as the “base” score the average SPD_{Vi} value of the class VS belonging to, the vulnerability score is calculated by adding to it the contributions of all the known parameters by the Equation 2.1

$$SPD = SPD_v + \sum_{s=1}^n q_s + \frac{\sum_{j=1}^m \sum_{i=1}^m (p_j + p_i)c_{ij}}{2m} \quad (2.1)$$

in which:

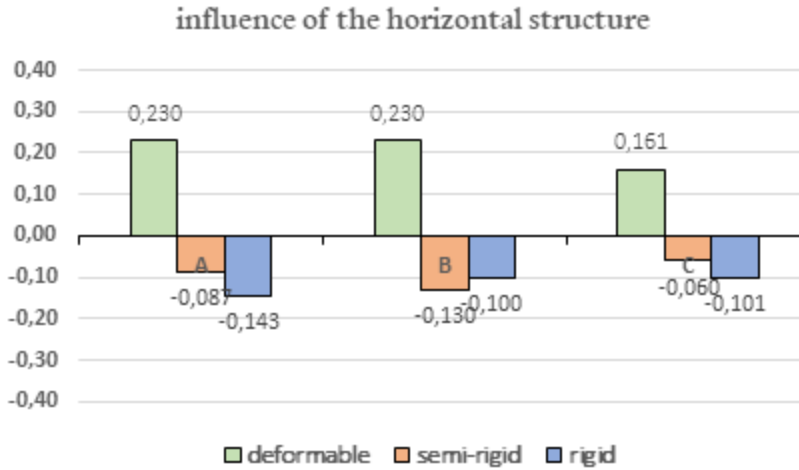


Figure 2.3: Example of influence of the horizontal structure in the vulnerability behaviour

- q is the influence of the independent parameter
- p is the influence of the dependent parameter
- n is the number of independent parameters
- m is the number of dependent parameters
- c_{ij} is the coefficient of correlation between p_i and p_j parameters

The coefficient of correlation c_{ij} takes into account the simultaneous occurrence of two considered parameters. It is possible, in fact, that choosing two variables of two parameters the obtained sample of buildings are similar. For example, there is a high probability that ancient buildings, pre 1919, have wooden floors. If

the sample of buildings is similar, the influence of the combined parameters is considered for two times. To avoid this problem, the coefficient of correlation between the parameters i and j is introduced, and it is defined as the probability of non-occurrence of the two parameters.

2.4 Seismic vulnerability assessment tools

2.4.1 The Damage Probability Matrices

Damage Probability Matrices represents the probability of a specific building typology to reach a fixed level of damage for discrete values of input, generally expressed in intensity. Pioneer of the DPMs, and generally of the vulnerability evaluation of the buildings, has been Whitman, that in 1973 proposed some in depth treatments on the correlations among buildings typologies, seismic input values (expressed in Modified Mercalli Intensity - MMI) and level of damage. His works already shows an high sensitivity to the seismic risk and its mitigation (in terms of damages and costs), although it's not expressed as the convolution of hazard, exposure and vulnerability yet. In the [22], in fact, is specifically presented a methodology for analyzing the costs and the risks associated with designing of tall buildings against earthquake, while aim of the [23] is to define a Seismic Design Decision Analysis (SDDA) to multistory buildings in Boston according to the Building Code for ZONE.

To these purposes the estimation of the probable behaviour of the considered buildings typologies in respect to considered input value is presented in the works, through damage probability matrices. In [22] the analyses are focused on the high rise buildings (5 or more stories) in the Los Angeles area hitten by the San Fernando earth-

SUMMARY OF BUILDING CATEGORIES

BUILDING TYPE	BUILDING HEIGHT	FOUNDATION TYPE	DESIGN STRATEGY
All types	All heights	All types	All buildings
Steel	5-7		Pre-1933
Concrete	8-13		1947-1971
	14-18		
	19+		

Figure 2.4: Buildings parameters considered by Whitman 1973

quake on 9 February 1971. The DPMs have been produced on the basis dataset in which about 1,500 buildings were collected by five different database (Original data base, BOMA Questionnaire, MIT Questionnaire, MIT/BOMA Questionnaire and Steinbrugge damage). The considered typological characteristics have been summarized in Figure 2.4. On the basis of these parameters and adopted design strategies, some specific buildings systems have been defined. The concept of the building system is, essentially, the precursor of the concept of vulnerability class. Furthermore, the work considers nine levels of damage (included no damage), that are resumed in Figure 2.5.

On the basis of these data and considering the input value in MMI, Whitman produced DPMs in the forms reported in Figure 2.6.

In 1982 the authors Braga, Dolce and Liberatore developed the first DPMs for the Irpinia event following the line adopted by Withman. The work was based on the information about damages detected on a statistical sample of 38,000 buildings. The damage distributions of each class of buildings corresponding to the different seismic intensities has been calculated on the basis of a binomial distribution. Also, three vulnerability classes (A, B, and C and) has been

EARTHQUAKE DAMAGE STATES			
	Description of Level of Damage	Damage Ratio* %	
		Central Value	Range
0	No damage	0	0-0.05
1	Minor non-structural damage--a few walls and partitions cracked, incidental mechanical and electrical damage	0.1	0.05-0.3
2	Localized non-structural damage--more extensive cracking (but still not widespread); possibly damage to elevators and/or other mechanical/electrical components	0.5	0.3-1.25
3	Widespread non-structural damage--possibly a few beams and columns cracked, although not noticeable	2	1.25-3.5
4	Minor structural damage--obvious cracking or yielding in a few structural members; substantial non-structural damage with widespread cracking	5	3.5-7.5
5	Substantial structural damage requiring repair or replacement of some structural members; associated extensive non-structural damage	10	7.5-20
6	Major structural damage requiring repair or replacement of many structural members; associated non-structural damage requiring repairs to major portion of interior; building vacated during repairs	30	20-65
7	Building condemned	100	65-100
8	Collapse	100	

* Ratio of cost of repair to replacement cost

Figure 2.5: Levels of damage defined by Whitman 1973

Chapter 2. The seismic vulnerability

GROUP CHARACTERISTICS: NUMBER OF BUILDINGS: 368. HEIGHT: 5 to 100 STORIES. AGE: 1800 to 1972. STRUCTURAL TYPE: ALL TYPES. FOUNDATION TYPE: ALL TYPES.

DAMAGE PROBABILITY MATRIX

DAMAGE STATE		MERCALLI INTENSITY		
	DAMAGE RATIO			
	UPPER BOUND			
STATE	(%)	VI	VII	VIII
0	0.05	80.5	25.1	6
1	0.3	15.6	24.7	19
2	1.25	3.9	26.2	44
3	3.5	2.7	14.2	13
4	7.5	0	5.8	6
5	20	0	2.5	12
6	65	0	1.5	0
7	100	0	0	0
NO. BUILDINGS		77	275	16

Figure 2.6: Example of damage probability matrix produced by Whitman 1973

Table 2.2: Damage probability matrices for vulnerability class A produced by Braga et al (1982)

Vulnerability class A						
I	D0	D1	D2	D3	D4	D5
VI	0.19	0.37	0.30	0.12	0.02	0.00
VII	0.06	0.23	0.34	0.25	0.09	0.01
VIII	0.00	0.02	0.11	0.29	0.38	0.20
IX	0.00	0.00	0.02	0.11	0.37	0.49
X	0.00	0.00	0.00	0.03	0.23	0.73

Table 2.3: Damage probability matrices for vulnerability class B produced by Braga et al (1982)

Vulnerability class B						
I	D0	D1	D2	D3	D4	D5
VI	0.36	0.41	0.18	0.04	0.00	0.00
VII	0.19	0.37	0.30	0.12	0.02	0.00
VIII	0.03	0.15	0.31	0.31	0.16	0.03
IX	0.00	0.02	0.11	0.29	0.38	0.19
X	0.00	0.00	0.02	0.11	0.37	0.50

introduced by the authors depending on the typological characteristics on the buildings and a DPM based on the MSK scale was evaluated for each class. Their contents have been summarized in the Tables 2.2, 2.3 and 2.4 for the vulnerability classes A, B and C respectively. The DPMs for the same seismic event has been also proposed by Zuccaro following the same principles, but the data have been subdivided in four vulnerability classes. In Figure 2.7 the data have been resumed.

Figure 2.7: Damage probability matrices produced by Zuccaro et al. 2000

vulnerability CLASS	I	Level of Damage					
		D0	D1	D2	D3	D4	D5
A	5	34%	41%	21%	4%	0%	0%
B		52%	36%	11%	1%	0%	0%
C		66%	29%	5%	0%	0%	0%
D		86%	13%	1%	0%	0%	0%
A	6	29%	41%	24%	6%	0%	0%
B		44%	39%	15%	2%	0%	0%
C		59%	33%	8%	0%	0%	0%
D		77%	20%	3%	0%	0%	0%
A	7	19%	38%	30%	11%	2%	0%
B		35%	41%	20%	4%	0%	0%
C		53%	36%	10%	1%	0%	0%
D		66%	29%	5%	0%	0%	0%
A	8	6%	24%	35%	25%	9%	1%
B		22%	39%	27%	10%	2%	0%
C		41%	39%	17%	3%	0%	0%
D		56%	34%	9%	1%	0%	0%
A	9	1%	7%	23%	35%	26%	8%
B		10%	30%	36%	19%	5%	0%
C		31%	40%	23%	6%	0%	0%
D		44%	39%	17%	0%	0%	0%
A	10	0%	2%	11%	30%	38%	19%
B		3%	16%	31%	31%	16%	3%
C		22%	39%	28%	10%	1%	0%
D		28%	41%	25%	6%	0%	0%
A	11	0%	0%	4%	18%	41%	37%
B		0%	2%	14%	31%	36%	17%
C		4%	18%	33%	30%	13%	2%
D		5%	20%	33%	28%	12%	2%
A	12	0%	0%	0%	0%	5%	95%
B		0%	0%	0%	2%	17%	81%
C		0%	0%	0%	4%	23%	73%
D		0%	0%	0%	5%	29%	66%

Table 2.4: Damage probability matrices for vulnerability class C produced by Braga et al (1982)

Vulnerability class C						
I	D0	D1	D2	D3	D4	D5
VI	0.71	0.25	0.03	0.00	0.00	0.00
VII	0.40	0.40	0.16	0.03	0.00	0.00
VIII	0.13	0.33	0.33	0.17	0.04	0.00
IX	0.05	0.21	0.34	0.28	0.11	0.02
X	0.00	0.05	0.18	0.34	0.31	0.11

2.4.2 The Vulnerability curves

The vulnerability curves of a building class represent the probability that a building of the class will reach a fixed damage level as the hazard changes. Mathematically, it can be described as $P[LD|H]$ i.e. as a function of the conditional probability of a fixed damage level for a fixed hazard value. The construction of the fragility curves for the particular structural system allows to estimate the degree of damage expected for each hazard level, thus representing the clearest, and also the most complete, conceptual way to estimate the vulnerability of the individual building.

The determination of vulnerability curves is different if an observational or analytical approach is used. In the first case, in fact, the curves are calibrated with a linear regression method starting from a dataset. Once a vulnerability class has been fixed and the distribution of buildings on the damage levels for each hazard value recorded, it is in fact possible to construct the representative curve of the damage indicated using the probability or average squared deviation method.

When the approach is analytical, on the other hand, the calibration of the vulnerability curves of a building class depends on the

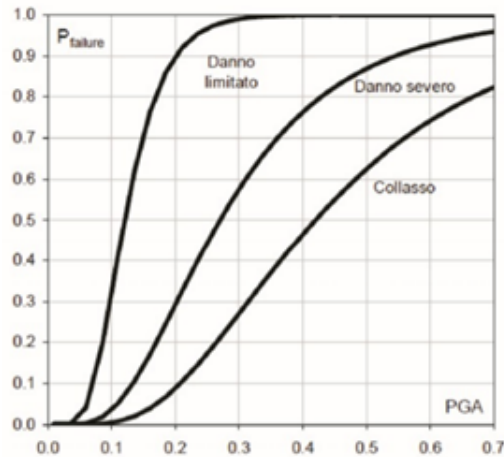


Figure 2.8: Example of vulnerability curve (Polese, 2002)

determination of the fragility curves of the structural system considered. An example of fragility curves constructed as a function of peak ground acceleration as a seismic hazard parameter (PGA) is shown in Figure 2.8 where three fragility curves obtained for the same structural system are simultaneously represented, each corresponding to a different limit state (insignificant damage; slight damage; severe damage). However, it is necessary to distinguish the case in which one wants to study a single building, taking into account all its details and characteristics that distinguish it, from the case in which one wants to study a sample of buildings of a certain area represented by a typological class.

In the first case, in fact, given the completeness and accuracy of the input data, it is possible to go to high levels of detail and obtain the fragility curves for data damage levels in an analytical way through numerical simulations on the seismic response of the building. In general, given the great burden of computation and modeling this

operation is aimed at buildings with particular strategic value or historical monuments. In the second case, instead, since we study a class of buildings that can be represented by macro-parameters such as shape, size, year of construction, etc., we end up studying a "medium" building in which there is the difficulty of considering, with an analytical approach, the influence of all macro-parameters on the seismic behavior of the structure. It is for this reason, the fragility curves of typological classes of buildings are empirically constructed by means of a statistical analysis of the data concerning the behaviour of buildings that can all be traced back to the same class.

2.4.3 Capacity spectrum method

The Hazus method (1999) can be considered a method that can be considered quantitative, although there is a component based on expert judgement and heuristic data. The method allows to calculate the probability that a class of structures suffers a fixed level of damage. The damage scale is divided into four boundary states: light, moderate, extended and total; for each of which a qualitative description is provided in relation to the different structural categories. In the probabilistic evaluation of the different degrees of damage that can occur, the variability of the seismic input and the variability of the capacity of the building class are taken into account. Building classes are identified by building type, number of floors and time of construction of the building.

The capacity of a "class" of buildings is expressed through the capacity curve, which expresses the lateral resistance of a building as a function of a significant lateral displacement. It is expressed in terms of acceleration and spectral displacement in order to easily compare the values of the curve with the seismic demand represen-

ted in response spectra. Its representation is similar to a push-over, but it is obtained in a simplified way, considering only two representative points: the capacity at the plastic limit and the ultimate capacity.

Seismic demand is assessed using the Capacity Spectrum Method (CSM). To obtain the spectral intensity parameter that defines the threshold for the level of collapse, the point of intersection of the capacity curve of a certain structural class with the fixed spectrum is considered, derived from the probabilistic seismic mapping of the territory, suitably reduced to take into account the non-linear behavior of the structure. The probability of reaching or exceeding predetermined limit states, assigned to be the "median" spectral response, is expressed by means of fragility curves with lognormal distribution.

2.4.4 Collapse mechanisms

The first analyses based on the collapse mechanisms has been proposed by D'Ayala and Speranza in 2002 with the methodology FaMIVE (Failure Mechanism Identification and Vulnerability Evaluation). The methodology is specific for the studies of historic masonry buildings. The procedure provides to define the low value of collapse multiplier for the in-plane and out-of-plane mechanisms that can occurs on the façades of the buildings.

Chapter 3

Empirical calibration of the vulnerability curves for Italian masonry buildings

3.1 Introduction

In this Chapter, the seismic vulnerability of Italian masonry buildings is evaluated adopting a critical observational approach based on the statistical analyses of damaged surveyed on Italian masonry buildings after past seismic events. The described approach aims to assess vulnerability curves, as a lognormal distribution in function of the acceleration, for Italian masonry buildings. To this purpose, a damage and typological Italian database has been exploited and, on the basis of statistical correlations among buildings typologies, damages and ground motion have been studied. As all empirical approaches, the study assumes that damage due to past earthquakes observed in the structures classified by type, will be the same in future earthquakes in the same region and also this

damage is representative of the vulnerability of areas having similar building stocks hit by a future seismic event with similar size.

The reliability of the curves, in the framework of Italian risk assessment at national scale, is connected to the large size of the database, in which about 240,000 buildings are collected. This database can carefully reflect the real damage and also incorporate the effects on building response of the factors difficult to model like material degradation, configuration and detailing arrangement.

The curves are developed in the framework of the technical board promoted by Italian Civil Protection with the aim to develop seismic vulnerability curves for Italian buildings differently classified in function of vertical structures (masonry and reinforced concrete) to assess scenario and risk analyses by IRMA platform (Italian Risk Map). The vulnerability curves have been derived using a regression method and their calibration has been supported by critical observations on the reliability of the dataset and, consequently, by introducing corrective assumptions.

3.2 Calibration

The steps adopted to calibrate the vulnerability curves exploiting the PLINIVS database have been: harmonization of the data; assignment of the vulnerability class to each building in the database; mathematical calibration of the vulnerability curves. The second step of the procedure provides to assign the vulnerability class through the S.A.V.E. procedure presented in the paragraph 2.3.2. Also, the last step has been done exploiting the procedure illustrated in Figure 3.1.

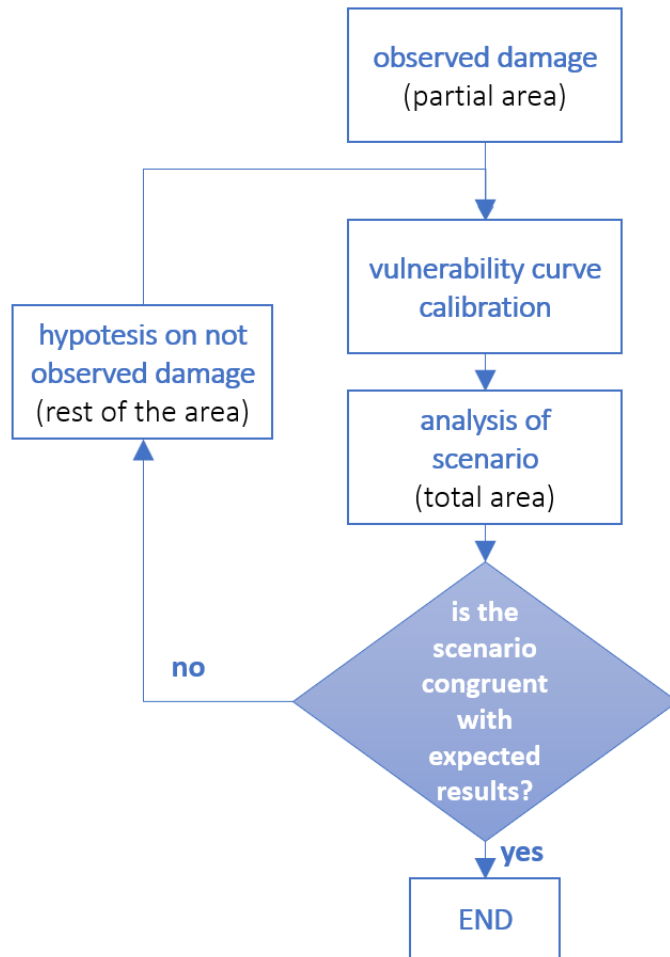


Figure 3.1: The adopted empirical procedure

3.2.1 Harmonization of the database

The PLINIVS database contains information on about 240,000 damaged masonry buildings collected for main Italian seismic events (Irpinia 1980, Abruzzo 1984, Umbria Marche 1997, Pollino 1998, Molise Puglia 2002, Emilia 2003, Aquila 2009, Emilia 2012). Survey activities have been done with different forms that differently organizes information about typological characteristics and levels of damage. In particular, four different forms have been used to collect data: the Irpinia Form for Irpinia 1980 event, the Abruzzo form for Abruzzo 1984 event, the Pollino form for the Pollino 1998 event and the AeDES form for the remaining events. In Appendix all the forms have been presented.

The first step of harmonization of the dataset provides to uniform (where possible) the nomenclature of the typological characteristics and to organize these information in classes of parameters. The outcomes of this work of harmonization has carried out the following list of parameters:

- **Vertical Structure:** generic masonry, irregular and weak masonry, regular and good quality masonry;
- **Horizontal Structure::** wooden floors, steel floors, brick concrete floors, vaults, mixed;
- **Number of floors:** 1 or 2, 3 or 4, 5 or 6, 7 or 8, more of 8;
- **Age of construction:** before 1919, 1919 - 1945, 1946 - 1961, 1962 - 1971, 1972 - 1981, after 1981;
- **Position of the building in the aggregate:** isolated, lateral, centred, corner;
- **Isolated pillars:** yes, no;

-
- **Horizontal connections:** yes, no;
 - **Plant regularity:** yes, no;
 - **Panels regularity:** yes, no;
 - **Roof:** light roof, light and of thrust type, light and no of thrust type, heavy roof, heavy and of thrust type, heavy and no of thrust type;
 - **Reinforcement:** no reinforce, steel reinforces, no steel reinforces.

With regard to the second harmonization step of the database, an unequivocal damage scale has been defined to which the formats of the survey forms could be attributed. In particular, the reference scale has been identified in the EMS98 guide, that introduces the following six levels of damage (no damage included):

- D0 - no damage;
- D1 - no structural damage, slight non-structural damage;
- D2 - slight structural damage, moderate non-structural damage;
- D3 - moderate structural damage, heavy non-structural damage;
- D4 - heavy structural damage, very heavy non-structural damage;
- D5 - very heavy structural damage.

Chapter 3. Empirical calibration of the vulnerability curves for Italian masonry buildings

Table 3.1: Conversion from damage reported in Irpinia Form and EMS98 damage

Entity of the damage	grade
no damage	1
not relevant damage - non-urgent repairable	2
light damage - repairable	3
considerable - to be partially cleared - repairable	4
serious - to be cleared - repairable	5
very serious - to be cleared and demolished	6
partial collapse - to be demolished	7
collapsed	8

The scales adopted by Irpinia, Abruzzo and AeDES forms and the meaning of each grade have been reported in the Tables 3.1, 3.2 and 3.3 respectively. On the basis of the definitions, the correspondence with the EMS98 scale have been considered as reported in 2.1.

With reference to the seismic input, the values of PGA for each municipality hit by the seismic event of L'Aquila 2009 have been retrieved by the INGV shakemap. For the others events,

Table 3.2: Conversion from damage reported in Abruzzo Form and EMS98 damage

Entity of the damage	grade
light damage	1
relevant damage	2
serious damage	3
very serious damage	4
destroyed	5

Table 3.3: Conversion from damage reported in AeDES Form and EMS98 damage

			vertical structure	horizontal structure
high	>2/3	A	5	5
	1/3 - 2/3	B	5	4
	<1/3	C	4	4
medium	>2/3	D	3	3
	1/3 - 2/3	E	3	3
	<1/3	F	3	3
light	>2/3	G	3	2
	1/3 - 2/3	H	2	2
	<1/3	I	2	1
no damage	-	L	0	0

the Macroseismic Intensity of the municipalities has been obtained by the DBMI-INGV site (<https://emidius.mi.ingv.it/DBMI/>), and after converted in PGA through the Margottini Law Conversion expressed in 3.1.

$$a = \frac{10^{0.525+0.22i}}{981} \quad (3.1)$$

3.2.2 Mathematical calibration of the vulnerability curves

The vulnerability curve represents the probability that a level of damage is reached or exceeded for a fixed value of hazard. In this work the vulnerability curves are obtained applying the minimum square regression method on the DPMs derived by the PLINIVS database. To this purpose, for each of the three vulnerability class

Chapter 3. Empirical calibration of the vulnerability curves for Italian masonry buildings

Table 3.4: Damage Probability Matrix of the masonry buildings for the vulnerability class A

		Vulnerability class A					
HAZARD		Level of damage					
		D0	D1	D2	D3	D4	D5
V	0.04	0.19	0.30	0.20	0.18	0.09	0.04
VI	0.07	0.12	0.30	0.16	0.21	0.13	0.08
VII	0.12	0.12	0.22	0.20	0.21	0.16	0.08
VIII	0.20	0.08	0.17	0.22	0.18	0.26	0.09
IX	0.33	0.06	0.12	0.21	0.18	0.27	0.17
X	0.54	0.10	0.14	0.12	0.18	0.26	0.19

(A, B and C) the building distribution on each PGA value has been estimated, and the cumulative values of each level of damage have been calculated. On the basis of these data, a regression method has been applied on the cumulative DPMs and the vulnerability curves depending on the surveys data only have been derived. Damage Probability Matrices (DPMs) associated to the PLINIVS database have been extracted from the data considering the correlations among the vulnerability class, the seismic input value and the level of damage. The DPMs have been summarized in Tables 3.4 , 3.5 and 3.6 for the vulnerability class A, B and C respectively. The seismic input is reported both in intensity (I) both in acceleration (PGA) .

On the basis of these data, continuous vulnerability functions depending on acceleration in the lognormal shape have been elaborated. To this purpose the minimum square regression method has been applied to the dataset, and the parameters of each vulnerability curve have been defined through the equation 3.2

$$find(\lambda, \beta) : \min[y_i - \log(x_i, \lambda, \beta)]^2 \quad (3.2)$$

in which

Table 3.5: Damage Probability Matrix of the masonry buildings for the vulnerability class B

Vulnerability class B							
HAZARD		Level of damage					
I	pga	D0	D1	D2	D3	D4	D5
V	0.04	0.25	0.37	0.21	0.11	0.04	0.02
VI	0.07	0.30	0.34	0.18	0.11	0.05	0.02
VII	0.12	0.28	0.33	0.21	0.10	0.06	0.02
VIII	0.20	0.18	0.25	0.25	0.15	0.15	0.03
IX	0.33	0.12	0.20	0.32	0.15	0.15	0.06
X	0.54	0.19	0.20	0.18	0.15	0.18	0.10

Table 3.6: Damage Probability Matrix of the masonry buildings for the vulnerability class C

Vulnerability class C							
HAZARD		Level of damage					
I	pga	D0	D1	D2	D3	D4	D5
V	0.04	0.32	0.44	0.14	0.07	0.03	0.01
VI	0.07	0.38	0.39	0.12	0.07	0.03	0.01
VII	0.12	0.45	0.33	0.13	0.06	0.04	0.01
VIII	0.20	0.31	0.33	0.17	0.08	0.09	0.02
IX	0.33	0.40	0.28	0.17	0.06	0.06	0.03
X	0.54	0.37	0.29	0.16	0.09	0.06	0.03

Chapter 3. Empirical calibration of the vulnerability curves for Italian masonry buildings

Table 3.7: Error measurement of the vulnerability curve of the class A (without revisions) in reference to the observed data

		Vulnerability class A				
HAZARD		square of the errors				
I	pga	D1	D2	D3	D4	D5
V	0.04	4.89E-3	9.97E-4	1.60E-6	1.99E-3	1.66E-4
VI	0.07	5.45E-3	1.14E-3	1.59E-3	3.68E-4	7.96E-4
VII	0.12	6.02E-4	3.31E-3	1.56E-4	1.16E-3	3.04E-5
VIII	0.20	5.77E-4	9.08E-3	3.39E-4	2.48E-4	2.84E-4
IX	0.33	2.87E-4	1.47E-2	1.91E-3	2.79E-3	4.62E-4
X	0.54	3.05E-3	1.84E-5	2.81E-6	2.14E-5	3.35E-5
S.R.S.S.		2.03E-2	2.85E-2	1.05E-2	1.35E-2	7.02E-3

- x_i is the PGA value;
- y_i is the cumulative distribution of the considered damage associated to the x_i value;
- λ is the logarithmic mean of the curve;
- β is the logarithmic standard deviation of the curve.

In Figures 3.2 - 3.4 the vulnerability curves for the classes A, B and C have been represented respectively, and scatter charts of the DPMs values have been overlaid. Furthermore, an estimation of the correspondence between the observed data (DPMs) and the continuous curves has been deepened. In particular, in the Tables 3.7, 3.8 and 3.9 for each acceleration value have been summarized the squares of the differences between the vulnerability curve value and observed data and for each vulnerability curve has been calculated the Square Root of the Sum of Squares value (S.R.S.S.). The high error has been founded in the D1 vulnerability curve of the class C, but it is lower than 5% so it can be considered that all the vulnerability curves have a good trend with observed data.



Figure 3.2: Vulnerability curves for Italian masonry buildings in class A - without assumptions

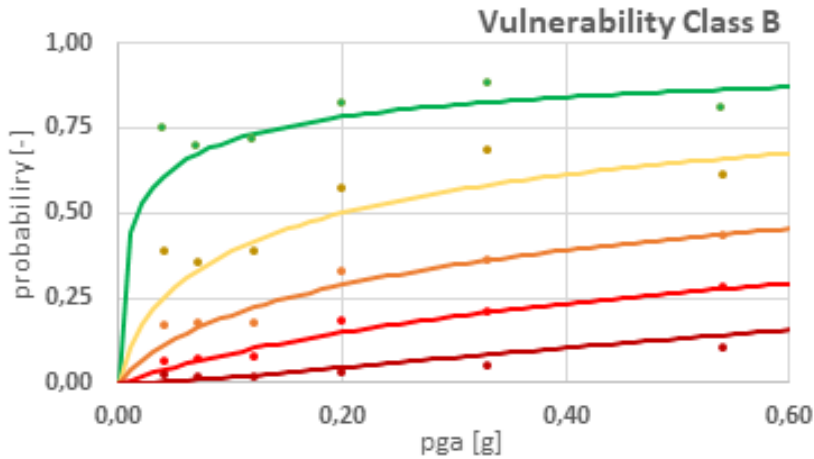


Figure 3.3: Vulnerability curves for Italian masonry buildings in class B - without assumptions

Table 3.8: Error measurement of the vulnerability curve of the class B (without revisions) in reference to the observed data

Vulnerability class B						
HAZARD		square of the errors				
I	pga	D1	D2	D3	D4	D5
V	0.04	2.00E-2	1.79E-2	3.69E-3	8.63E-4	4.53E-4
VI	0.07	5.36E-4	5.94E-4	3.14E-4	9.66E-5	1.10E-4
VII	0.12	2.00E-4	6.41E-4	1.77E-3	5.17E-4	2.31E-5
VIII	0.20	1.55E-3	5.74E-3	1.53E-3	1.03E-3	1.38E-4
IX	0.33	3.47E-3	1.07E-2	2.22E-6	3.89E-6	7.87E-4
X	0.54	2.92E-3	2.26E-3	1.91E-5	2.97E-5	1.38E-3
S.R.S.S.		2.82E-2	3.24E-3	1.43E-2	8.40E-3	8.96E-3

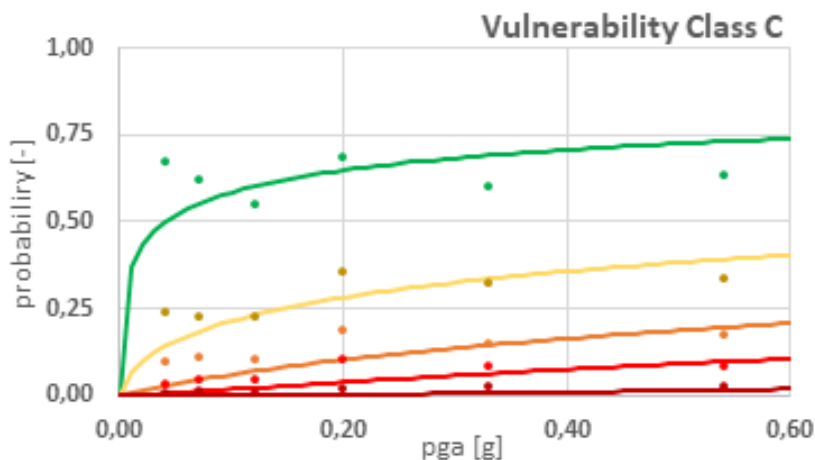


Figure 3.4: Vulnerability curves for Italian masonry buildings in class C - without assumptions

Table 3.9: Error measurement of the vulnerability curve of the class C (without revisions) in reference to the observed data

Vulnerability class C						
HAZARD		square of the errors				
I	pga	D1	D2	D3	D4	D5
V	0.04	3.17E-2	9.13E-3	5.13E-3	6.73E-4	3.89E-5
VI	0.07	4.84E-3	1.88E-3	4.38E-3	1.05E-3	1.34E-4
VII	0.12	2.33E-3	1.19E-5	1.05E-3	5.18E-4	1.02E-4
VIII	0.20	1.41E-3	5.80E-3	6.98E-3	4.62E-3	3.47E-4
IX	0.33	7.98E-3	1.58E-4	2.38E-5	6.15E-4	3.33E-4
X	0.54	9.45E-3	2.58E-3	2.92E-4	1.32E-4	9.49E-5
S.R.S.S.		4.00E-2	2.33E-2	2.23E-2	1.46E-2	5.40E-3

However, although the errors summarized in the Tables 3.7, 3.8 and 3.9 can be considered acceptable, some critical remarks have to be done on the reliability of the DPMs dataset. In fact, the accuracy of the distribution of the damage level building is strictly related to the completeness of the detection at each seismic input value. Generally, when the seismic input value is low, less accuracy is associated to the building distributions because there is a high probability that buildings have been not damaged and no survey activities have been done. This problem has been highlighted since first empirical works on collected data: in [?] the author reports: “While cases of heavy damage to multi-story buildings have been well documented, there is little or no documentation on such buildings with no damage or only very light damage”.

To overcome the problem of wrong calibrations of the vulnerability curves, three assumptions have been introduced to correct the trend. The first one consists into weigh the reliability of the data (i. e. the buildings distribution on the level of damage) for each seismic input value on the basis of the associated comprehensiveness of the survey activity. To this purpose, the Completeness Index I_c of the survey activity for each input value has been introduced, and it has been defined as the percentage of surveyed buildings compared to the total area invested by the considered input value. In this work, the Completeness Index I_c has been estimated in reference to data on the L’Aquila 2009 event only, since its best completeness on data. Required information are: the input value, the total number of buildings in the affected area and the number of surveyed buildings. The input value has been derived by the shakemap of the INGV, in which PgA values are furnished through iso-acceleration curves with steps of 0.02 g. The total number of buildings in the affected data has been derived by the ISTAT 2001 database, in which the total number of buildings is furnished for

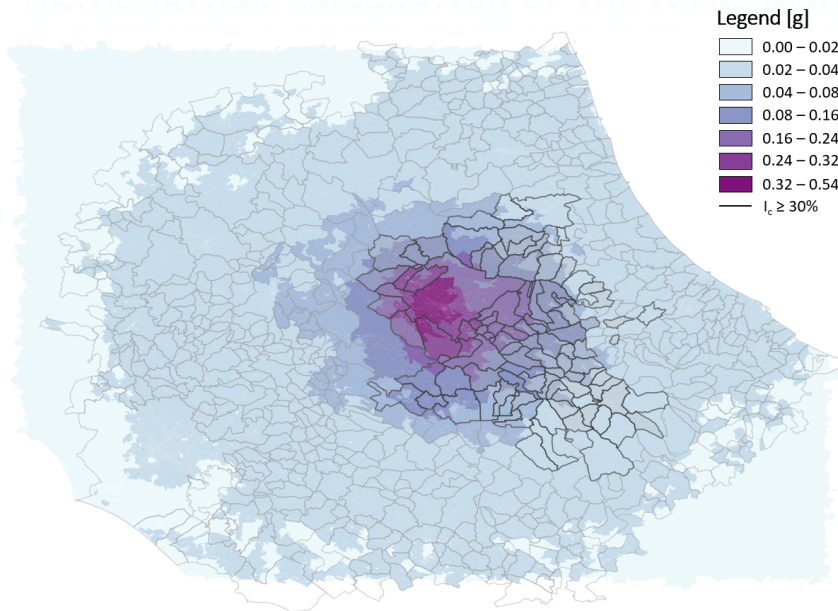


Figure 3.5: L'Aquila shakemap

unit zones. The number of surveyed buildings has been provided by the PLINIVS database for each municipality. Since the inventory of buildings stored in the PLINIVS database is grouped by municipalities, in order to harmonize the information, the ISTAT2001 data, provided by census zones, have been grouped by single municipalities. Furthermore, a single value of PGA has been associated to each considered municipality; in particular, it is obtained considering the PGA value of the L'Aquila 2009 shakemap (Figure 3.2.2) corresponding to the centroid of the municipality.

For each step of PGA, all associated municipalities have been considered and the number of surveyed buildings (by PLINIVS data-

base) and the number of total buildings (by ISTAT2001 database) have been evaluated. At the end, the Completeness Index I_c on the L'Aquila2009 sample has been calculated. This value, representative of the reliability of the data, has been introduced in the regression by correcting the equation 3.2 in the equation 3.3

$$find(\lambda, \beta) : \min I_c [y_i - \log(x_i, \lambda, \beta)]^2 \quad (3.3)$$

The outcomes show that at lower values of seismic input corresponds lower values of I_c , since lower hazard generates less damages and, probably, no damaged buildings have been neglected. “No information” at lower seismic values can be considered, in fact, as a “no necessary information” for the surveyors, i.e. absence of damage. On the basis of these considerations, the second assumption has been introduced, that considers the absence of data for low acceleration values ($PGA \leq 0,03$ g). In particular, it is considered that all no detected buildings in vulnerability classes B and C have no damage (D0), the 30% of no detected buildings in vulnerability class A have a no structural damage (D1) and the remaining 70% have no damage (D0).

At the end, the last conceptual assumption takes into account that vulnerability curves representative of different levels of damage but belong to the same class cannot have intersection points. To avoid mathematically the problem, the same logarithmic standard deviation has been assumed for curves of the same vulnerability class. In Figures 3.6 - 3.8 the updated vulnerability curves for the classes A, B and C respectively have been represented, and scatter charts of the DPMs values have been overlaid. Furthermore, analogous to the previous case, in Tables 3.10 - 3.12 have been summarized the squares of the differences between the vulnerability curve value and observed data for each acceleration value,

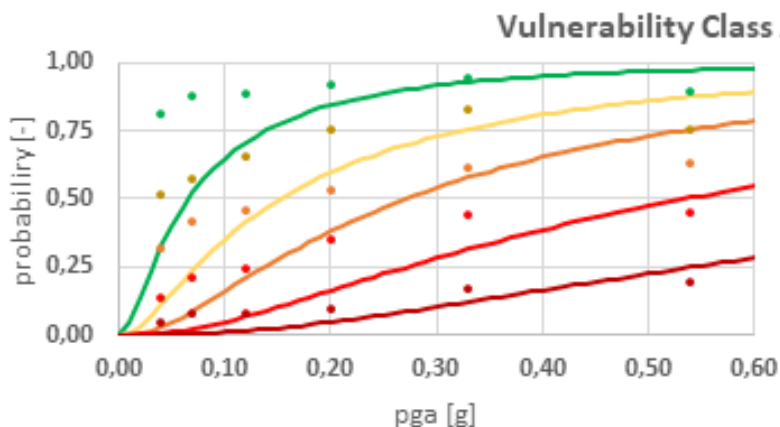


Figure 3.6: Vulnerability curves for Italian masonry buildings in class A - with assumptions

and furthermore the Square Root of the Sum of the Squares value (S.R.S.S.) for each vulnerability curve has been calculated.

It is shown that very high error values can be found especially in the D1 curves: the error is of the 24% for the class A and of 45% for the classes B and C. It is, also, shown that in all the classes high error values are estimated for low levels of damage than for high ones, and that the error decreases as the acceleration value increases.

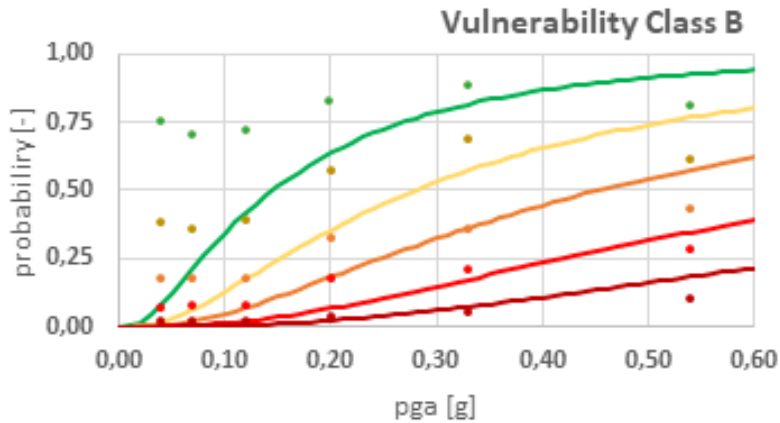


Figure 3.7: Vulnerability curves for Italian masonry buildings in class B - with assumptions

Table 3.10: Error measurement of the vulnerability curve of the class A (with revisions) in reference to the observed data

Vulnerability class A						
HAZARD		square of the errors				
I	pga	D1	D2	D3	D4	D5
V	0.04	2.36E-1	1.61E-1	8.17E-2	1.73E-2	1.84E-3
VI	0.07	1.27E-1	1.14E-1	1.11E-1	3.54E-2	5.54E-3
VII	0.12	3.03E-2	6.10E-2	6.34E-2	3.17E-2	4.42E-3
VIII	0.20	5.91E-3	2.39E-2	2.22E-2	3.47E-2	2.01E-3
IX	0.33	2.45E-4	4.73E-3	1.58E-3	1.62E-2	2.66E-3
X	0.54	5.96E-3	1.42E-2	1.49E-2	2.79E-3	2.81E-3
S.R.S.S.		1.06E-1	1.03E-1	9.04E-2	6.19E-2	2.31E-2

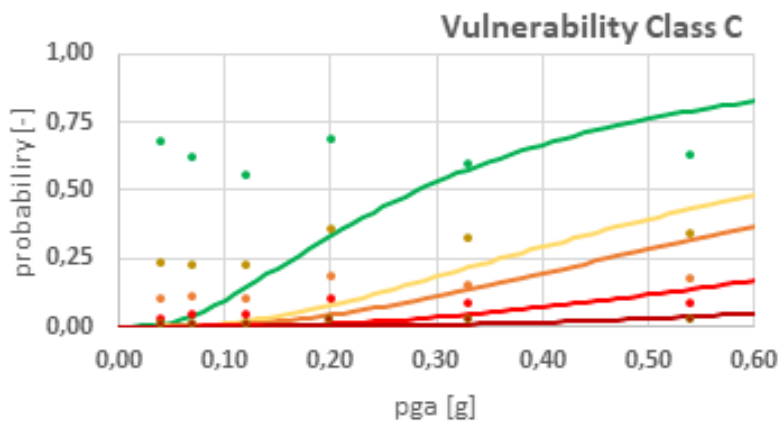


Figure 3.8: Vulnerability curves for Italian masonry buildings in class C - with assumptions

Table 3.11: Error measurement of the vulnerability curve of the class B (with revisions) in reference to the observed data

Vulnerability class B						
HAZARD		square of the errors				
I	pga	D1	D2	D3	D4	D5
V	0.04	4.54E-1	1.38E-1	2.89E-1	4.52E-3	6.11E-4
VI	0.07	2.38E-1	8.68E-2	2.59E-2	4.99E-3	3.69E-4
VII	0.12	9.15E-2	4.73E-2	1.0E-2	3.52E-3	1.53E-4
VIII	0.20	3.43E-2	4.89E-2	2.11E-2	1.30E-2	1.27E-4
IX	0.33	4.73E-3	1.27E-2	1.74E-8	1.34E-3	3.07E-4
X	0.54	1.37E-2	2.41E-2	2.07E-2	4.02E-3	6.16E-3
S.R.S.S.		1.52E-1	9.97E-2	5.50E-2	2.95E-2	1.46E-2

Table 3.12: Error measurement of the vulnerability curve of the class C (with revisions) in reference to the observed data

		Vulnerability class C				
HAZARD		square of the errors				
I	pga	D1	D2	D3	D4	D5
V	0.04	4.49E-1	5.67E-2	9.81E-3	1.00E-3	4.01E-5
VI	0.07	3.38E-1	5.06E-2	1.22E-2	1.94E-3	1.41E-4
VII	0.12	1.69E-1	4.35E-2	8.88E-3	2.20E-3	1.20E-4
VIII	0.20	1.25E-1	7.84E-2	2.10E-2	9.39E-3	2.96E-4
IX	0.33	6.58E-4	1.17E-2	1.89E-4	1.97E-3	2.96E-4
X	0.54	2.44E-3	8.25E-3	1.87E-2	2.58E-3	1.29E-4
S.R.S.S.		1.75E-1	8.32E-2	4.43E-2	2.29E-2	5.63E-3

3.3 L'Aquila 2009: a validation of the outcomes calculated through the IRMA platform

To test the proposed vulnerability curves, the impact scenario consequent to the L'Aquila earthquake 2009 has been assessed through the IRMA tool. For the hazard values, the platform exploits the INGV shakemap of the L'Aquila 2009 event and assigns to each municipality the pga value corresponding to the centroid of its geometry. The exposure values are estimated by IRMA through the correlations among three typological parameters (vertical structure, number of floors, age of construction) of the ISTAT2001 database and the distribution of the buildings on the three vulnerability classes A, B and C introduced by the user. The vulnerability parameters have been introduced through mean and standard deviation of the estimated curves. Furthermore, to avoid overstatement problems in areas with low values of PGA, the platform considers a cut

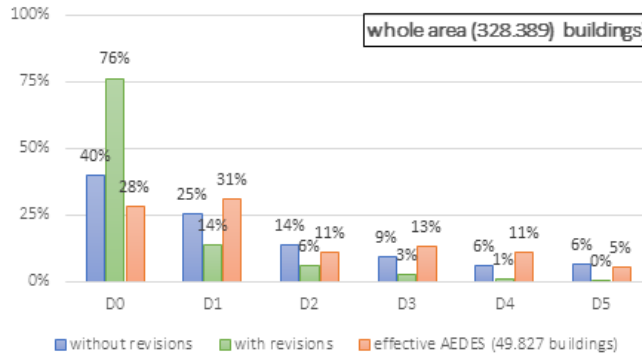


Figure 3.9: buildings distribution on the levels of damage in reference to the whole area and the effective AEDES forms

off of the curves for $PGA \leq 0,03 \text{ g}$.

On the basis of these parameters, the buildings distributions on the levels of damage caused by the L' Aquila seismic event through the two vulnerability approaches have been calculated. The outcomes are summarized in Figures 3.9 - 3.13. In particular, Figures 3.9 - 3.10 refer to the outcomes on the whole area invested by the earthquake.

In Figure 3.9 the buildings distribution on the basis of the AEDES form is estimated considering the *effective* surveyed buildings only, that are 49.827 on the 328.389, i. e. the 17% of the total buildings. Keeping the assumption on accuracy, it can be considered that the reliability of the data is under the 20%, so very low. Figure 3.10 shows the outcomes of the two approaches compared to the *integrated* AEDES, i. e. it is considered that the 20% of the not detected buildings have a level of damage equal to D1 and the remaining 80% is not damaged. It is shown that in the first case there is more similarity of outcomes between the AEDES forms

Chapter 3. Empirical calibration of the vulnerability curves for Italian masonry buildings

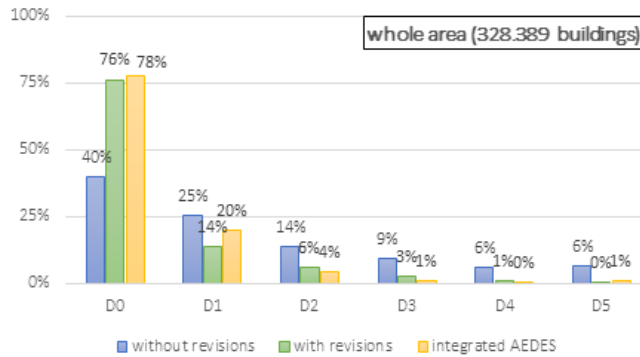


Figure 3.10: buildings distribution on the levels of damage in reference to the whole area and the integrated AEDES forms

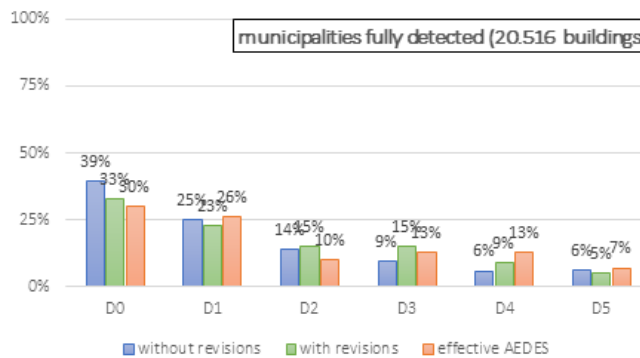


Figure 3.11: buildings distribution on the levels of damage in reference to the municipalities fully detected

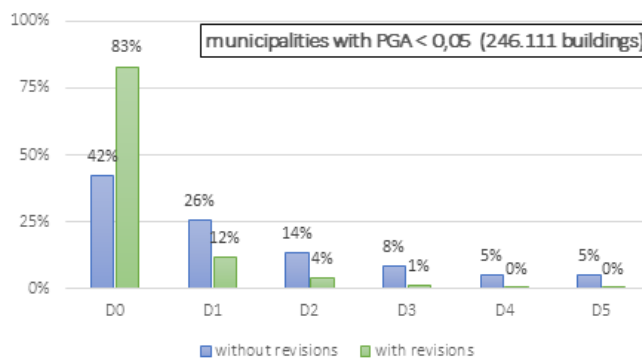


Figure 3.12: buildings distribution on the levels of damage in reference to the municipalities with $pga < 0.05g$

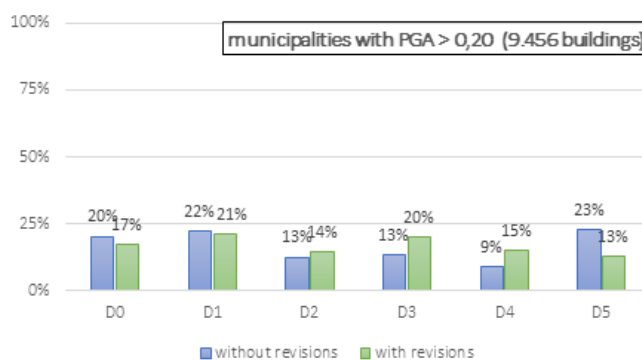


Figure 3.13: buildings distribution on the levels of damage in reference to the municipalities with $pga > 0.20g$

Chapter 3. Empirical calibration of the vulnerability curves for Italian masonry buildings

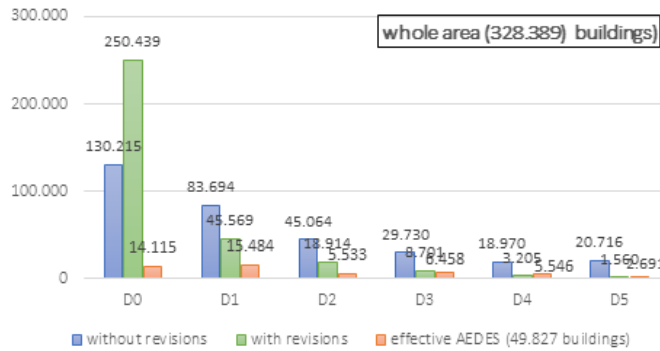


Figure 3.14: number of buildings on the levels of damage in reference to the whole area

and the “without revisions” model, instead in the second case the affinity is more evident between the integrated AEDES form and the “with revisions” model. Figure 3.11 shows the buildings distribution on the levels of damage calculated through the two models and the observed data for municipalities fully detected by AEDES forms. It is evident that both the models have a good compatibility with the data.

Furthermore, a comparison between the two models only is shown in Figures 3.12 - 3.13, in which damage buildings distribution is calculated for municipalities with $PGA < 0.05g$ and $PGA > 0.20g$, respectively. It is shown that high discrepancies can be recorded for low levels of damages and low PGA values, and on the contrary less differences can be found for high PGA values in all levels of damage, this is obviously justified by the assumptions of the “with revisions” method.

At the end, Figure 3.14 summarizes the number of buildings in each level of damage with reference to the whole area. A significant result that must be highlighted is that there is more accord-

ance of collapsed buildings between the “with revisions” model and the effective AEDES forms. An analysis of the errors of both methods in reference to effective AEDES forms shows that: both methods overestimate the number of no damaged buildings (D0), but the error of the “with revision” method in reference to the AEDES form is higher; the “without revisions” method overestimates significantly the high levels of damage (D3-D5). This shows that the “with revisions” method is more reliable because while it is reasonable that the AEDES forms are not compiled for undamaged buildings (D0), it is very unlikely that for very damaged buildings (D4-D5) the forms (which is the basis of requests for contributions for seismic improvement and adaptation measures) are not compiled. Furthermore, it is important to note that the “with revisions” method slightly underestimates the number of buildings with high damage levels (D4-D5), but this is caused by the intrinsic error of ISTAT 2001 database which, by confusing buildings and aggregates, provides a smaller total number of buildings than effective.

Chapter 3. Empirical calibration of the vulnerability curves for Italian masonry buildings

Chapter 4

Seismic behaviour of masonry buildings, out of plane and in plane, through limit state and D.E.M. analyses

4.1 Introduction

Seismic global behaviour of an unreinforced masonry building strictly depends on the combination of the typological vulnerability factors of the considered structure (quality of the masonry, typology and stiffness of the floor, typology and stiffness of the roof, connection among orthogonal walls, connection among bearing-walls and horizontal structures, etc). The collapse of a structure can be reached for

- **Global mechanisms of collapse:** the mechanism involves the structure as a whole. Before the collapse, the structure

reached a state of cracking that compromised the equilibrium of the entire system.

- **Local mechanisms of collapse:** : the mechanism involves marginal parts of the structure but their evolution, even if determines the collapse of a single element, does not involve the whole structural equilibrium.

MEDEA, a tool developed by the PLINIVS Study Centre for Civil Protection, contains a catalogue describing the mechanisms of global collapse of masonry and reinforced concrete buildings. The main global mechanisms related to masonry reported in the tool are shown in Figure 4.1. The effective collapse of a structure always occurs through the overturning of a facade or of one of its part, out of its geometric plane. This kinematic mechanism, however, can be activated after that the walls connected to the overturning facade are no longer able to resist to the seismic forcing that strikes the structure. When the resistance of these walls is remarkably low, or if the connections among the walls is not able to create an efficient interaction, it is possible to simplify the analysis considering the kinematic aspects only on the façade invested by the out of plane seismic force. This case is quite recurrent for very vulnerable buildings, defined as class A buildings. In literature, many treatments study these cases through the kinematic theorem of the limit analysis in which a collapse multiplier is estimated exploiting the Virtual Work Principle written for the considered mechanism analysed. A series of surveys on buildings collapsed as a result of seismic events have shown that the mechanisms that most frequently lead to the collapse of the structure are the simple overturning, the overturning for vertical flexion and the overturning for horizontal flexion. In the first part of this Chapter, the procedure to analyse the façade behaviour exploiting the limit analysis for

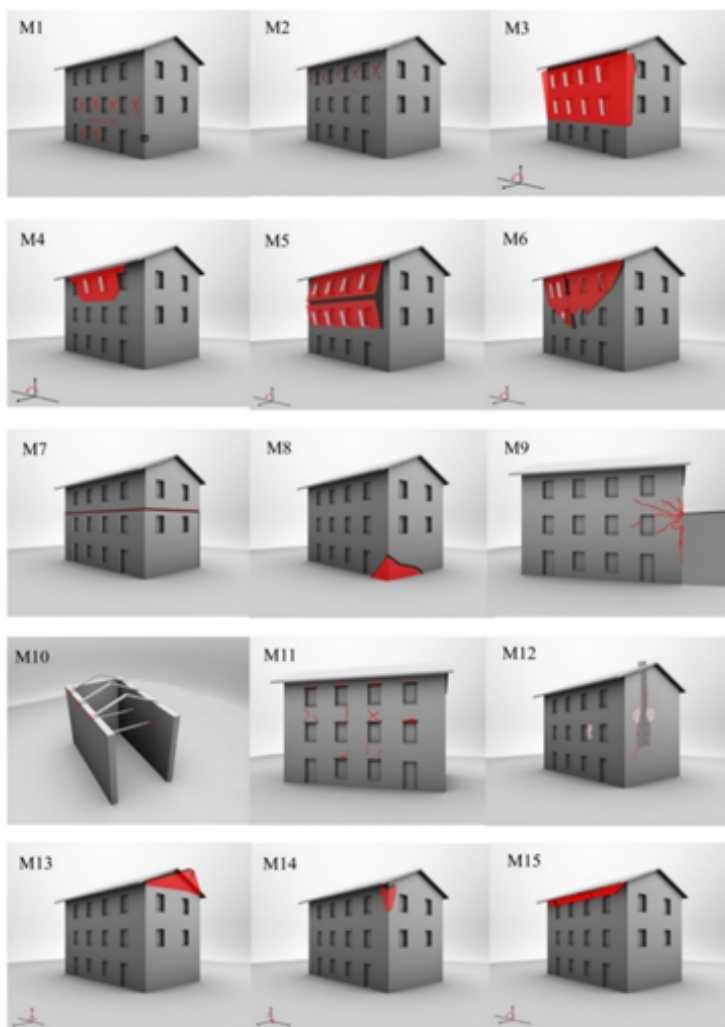


Figure 4.1: Global mechanisms of collapse for the masonry buildings according to Medea

these three collapse mechanisms. In the second part of this work is described the methodology used to define the in plane behaviour, with the aim to investigate the contribution of walls to resistance with reference to the seismic actions. To this purpose, a discrete element analysis (micro-modelling) has been used on walls made of rigid bricks and regular texture. Within the model, the crisis of the wall can only be reached by the breakage of the mortar and the consequent sliding between the bricks. Surveys were conducted on the formation and quantity of dislocations that are formed on the walls involved for resistance to the growth of seismic force. Afterwards, threshold limit values were defined for wall dislocations and for the identification of damage levels.

4.2 Model of the out of plane behaviour - Limit analysis

In the first part of this Chapter has been described the used methodology to evaluate the out of plane behaviour of the masonry walls under seismic actions. To this purpose a study based on the limit analysis for masonry structures has been adopted, combining the equilibrium condition of the wall with its potential kinematism. The masonry blocks are considered as rigid.

The Heyman assumptions are on the basis of the treatment: no tensile strength, infinite compressive strength and no sliding failure. In the analyses a single wall of the structure is considered and all the connected elements are modelled as applied forces. The applied loads are the permanent ones (verticals P_i and horizontals F_i) and the seismic ones (horizontal only) that are obtained multiplying the vertical permanent ones with a factor α_i .

A configuration of the wall is defined *cinematically possible* if it

guarantees that the work produced by the loads P_i , F_i and $\alpha_i P_i$ and the internal work associated to the deformations are equals. However, considering that rigid blocks have been assumed, the internal work of the wall is equal to zero. The lower value α able to activate the kinematism is defined as the collapse multiplier. Its evaluation can be done through the calculation of the virtual work theorem as in the equation 4.1, in which x and y represent the horizontal and vertical coordinates of the point in which is applied the considered force in respect to the rotation center.

$$\sum_i P_i \cdot x_{P_i} + \sum_i F_i \cdot y_{F_i} + \alpha \sum_i y_i \cdot u_{P_i} = 0 \quad (4.1)$$

According to the MEDEA tool, a methodology developed by the Italian Civil Protection with the aim to evaluate damages caused by seismic actions on masonry and R.C. buildings, the determination of the collapse multiplier has been specialized for the most common out of plane mechanisms: simple overturning, vertical bending, horizontal bending. In particular, for each considered kinematism the hinge configuration has been adopted and the virtual work theorem has been used to estimate the multiplier. In the evaluations the following quantities has been considered.

- α is the collapse multiplier;
- W_i is the weight of the wall i ;
- F_{Vi} is the vertical component of the vault on the floor i ;
- F_{Hi} is the horizontal component of the vault on the floor i ;
- P_{Si} is the weight of the floor on the wall i ;
- N is a generic vertical load on the wall i ;

Chapter 4. Seismic behaviour of masonry buildings, out of plane and in plane, through limit state and D.E.M. analyses

- P_H is the horizontal contribute of the roof;
- T_i is the action of the tie on the wall i ;
- s_i is the thickness of the wall i ;
- h_i is the vertical distance of the floor i or the tie i from the hinge;
- L_i is the length of the element i ;
- x_{G_i} is the horizontal distance of the weight of the element i from the hinge;
- y_{G_i} is the vertical distance of the weight of the element i from the hinge;
- d is the horizontal distance of the generic vertical load on the element i ;
- a_i is the horizontal distance of the generic vertical load on the element i ;
- h_{V_i} is the vertical distance of the horizontal force of the vault i ;
- d_{V_i} is the horizontal distance of the vertical force of the vault i ;

At the end, the corresponding a_g value of the trigger seismic base acceleration has been computed through the equation 4.2

$$a_g = \frac{\alpha q}{S} g \quad (4.2)$$

where:

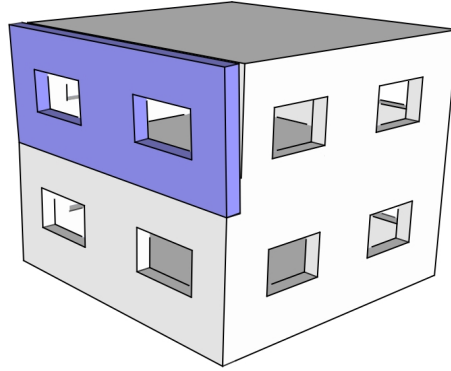


Figure 4.2: Simple overturning of one floor in a buildings with more floors

- α is the collapse multiplier;
- q is the ductility factor;
- S is the subsoil factor;
- g is the gravity acceleration.

4.2.1 Simple overturning

The simple overturning kinematism consist in a rigid rotation of a façade around a hinge on the basis or in the middle of the wall (Figures 4.2 and 4.3 respectively). In Figure 4.4 the kinematism has been represented in the transverse vertical section assuming a counter-clockwise rotation.

On the basis of the quantities reported in Figure 4.4, the multiplier α able to activate the mechanisms can be calculated through the equation 4.3.

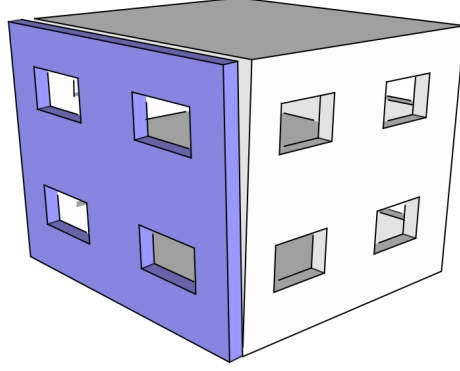


Figure 4.3: Simple overturning of the wall

$$\alpha = \frac{\sum_i (W_i \frac{s_i}{2} + F_{V_i} d_{V_i} + P_{S_i} d_i + T_i * h_i - F_{H_i} h_{V_i} - P_{H_i})}{\sum_i W_i y_{G_i} + F_{V_i} h_{V_i} + P_{S_i} h_i} \quad (4.3)$$

4.2.2 Vertical bending

The vertical bending kinematism involves in a vertical instability of the wall induced by the seismic inertial forces and the action of an intermediate floor (Figure 4.5). Rarely, it can be activated on one floor since the inertia of the wall (Figure 4.6). In the first case, the hinge is located in correspondence of an intermediate floor, while in the second case is on a point of an interstorey wall.

Figures 4.8 and 4.7 respectively show the cases in a section view. On the basis of the quantities reported in Figures 4.8 and 4.7 respectively, the multiplier α able to activate the mechanisms can be calculated through the equations 4.4 and 4.6. The quantity E in the equation 4.4 has been reported in the equation 4.5.

$$\alpha = \frac{E}{W_1 y_{G_1} + F_{V_1} h_{V_1} + P_{S_1} h_P + (W_2 y_{G_2} + F_{V_2} h_{V_2}) \frac{h_1}{h_2}} \quad (4.4)$$

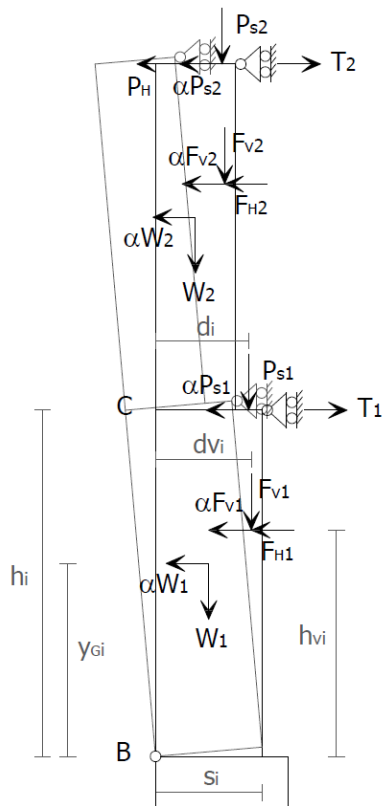


Figure 4.4: Simple overturning - a section view

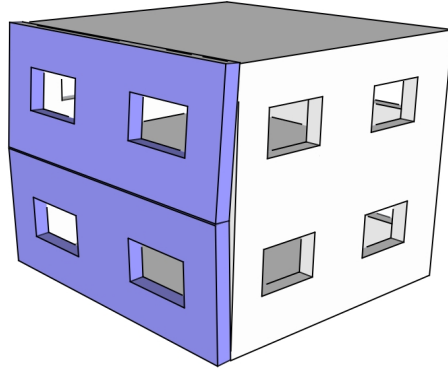


Figure 4.5: Vertical bending for a building of two floors

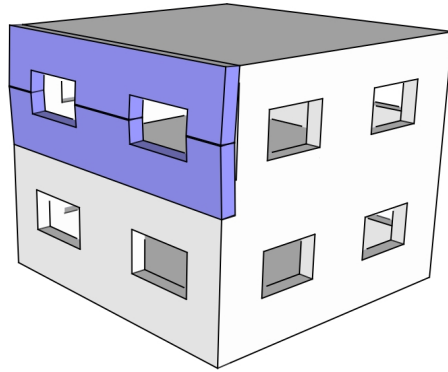


Figure 4.6: Vertical bending for one floor

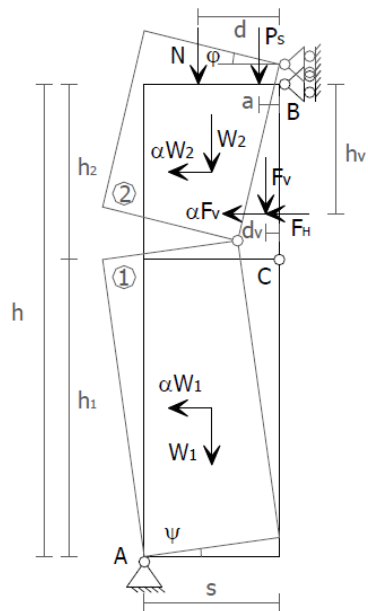


Figure 4.7: Vertical bending for one floor, a section view

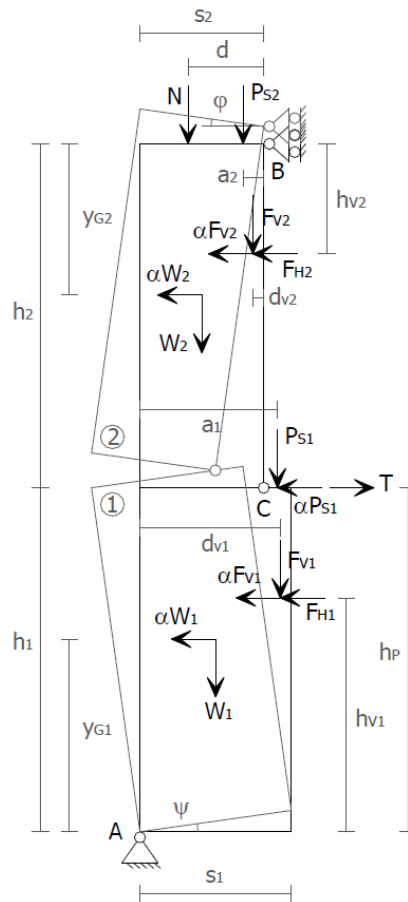


Figure 4.8: Vertical bending for two floors, a section view

$$\begin{aligned}
E = & \frac{W_1}{2}s_1 + F_{V_1}d_{V_1} + (W_2 + P_{S_2} + N + F_{V_2})s_2 + \\
& + \frac{h_1}{h_2}\left(\frac{W_2}{2}s_2 + P_{S_2}a_2 + Nd + F_{V_2}d_{V_2} - F_{H_2}h_{V_2}\right) + \\
& + P_{S_1}a_1 - F_{H_1}h_{V_1} + Th_P
\end{aligned} \tag{4.5}$$

$$\alpha = 2 \frac{(\mu - 1)(Nd + P_S a + F_V d_V - F_H h_V) + s(W + NP_S + F_V)}{(\mu - 1)(W_{\mu}^h + 2F_V h_V)} \tag{4.6}$$

4.2.3 Horizontal bending

The horizontal bending mechanism refers to two adjacent panels and it is related to arch mechanisms induced, within the wall sections, by out-of-plane actions (Figure 4.9).

In such a case, three hinges, as reported in Figure 4.10, are considered. Moreover, a horizontal force accounting for architectural constraints, such as the action of steel ties has to be considered.

On the basis of the quantities reported in Figure 4.10, the multiplier α able to activate the mechanisms can be calculated through the equation 4.7.

$$\alpha = \frac{H \cdot s(1 + \frac{L_1}{L_2}) - \sum_i (P_{H_{i1}}d_{i1} + P_{H_{i2}}d_{i2})}{W_1 x_{G_1} + W_2 \frac{L_1}{L_2} x_{G_2} + \sum_i (P_{V_{i1}}d_{i1} + P_{V_{i2}}d_{i2} \frac{L_1}{L_2})} \tag{4.7}$$

4.3 Model of the in plane behaviour - D.E.M. analysis

In this second part of the chapter, the adopted methodology used to estimate the in plane behaviour, under a seismic action, of a

Chapter 4. Seismic behaviour of masonry buildings, out of plane and in plane, through limit state and D.E.M. analyses

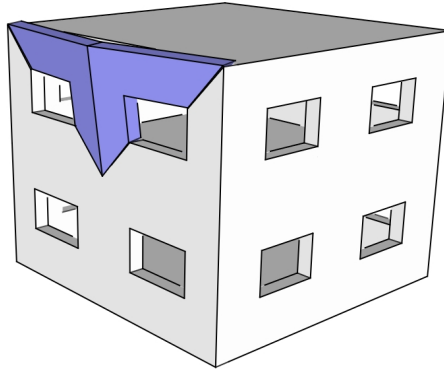


Figure 4.9: Horizontal bending phenomena

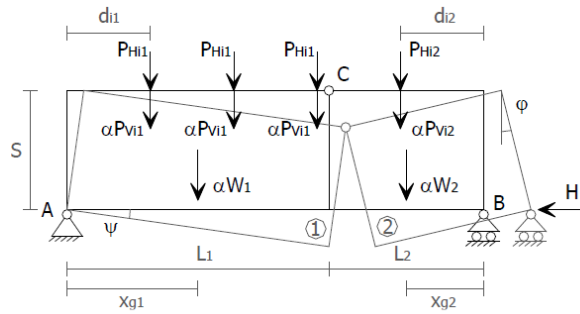


Figure 4.10: Horizontal bending, a section view

good quality wall masonry is presented. A micro-modelling has been used that through a discrete element method describes the kinematic and static configuration of each part of the studied wall. This model is specific for good designed wall masonry, since their ability to oppose to the out of plane kinematism, so rigid blocks regularly disposed have been considered to create the façade. Since rigid blocks have been assumed, the crisis of the wall under seismic actions can occur statically for the breackage of the mortar and, consequently, kinematically for the sliding of the bricks. The interaction among the elements is represented through a stiffness matrix, and its quantities are estimated on the basis of the mortar properties (i.e. mechanical characteristics and geometry).

The built method exploits a dynamic analysis. The period of the seismic sollecitation is discretized in time steps compatibles with the frequencies of the elements of the system, and for each time step the Newmark Method is applied. The Newmark Method calculates for each step the final kinematic quantities (displacements, velocities and accelerations) of each element of the wall on the basis of the initial ones and of the increments of the external forces in the considered time. The external forces applied on the wall are representative of the seismic actions only. In this work, horizontal seismic actions that linearly increases in the time have been considered. In particular, its increment in each time step has been defined as percentage of the gravitational forces or vertical loads applied to each element.

Starting from the kinematic values estimated for the rigid blocks, the tensile configuration in the mortar in each time step is calculated and a check of the sollicitation with the limit tension values of the mortar is done. On the basis of this check, i. e. the verification of eventual cracks in the mortar and new disposition of the blocks, the interaction among the elements is updated through new

stiffness and frictional laws adopted for the subsequent step.

At the end, the achievement of a level of damage is defined on the basis of the percentage of cracks on the masonry wall and the reciprocal distance between contiguous elements. In particular, when the condition of equilibrium between two contiguous elements cannot be verified, the kinematism is activated and the analysis stops. In particular, when the condition of equilibrium between two contiguous elements cannot be verified, the kinematism is activated and the analysis stops.

4.3.1 The wall discretization

The discrete element analysis proposed in this work has the aim to define the *in-plane* behaviour of a façade of a building under a seismic action. Both solicitation both the investigated behaviour of the wall are in the plane of the façade, so a 2D model has been adopted. Also, since good designed masonry only has been considered, the wall has been subdivided in single rectangular bricks with a regular pattern, and modeled as rigid blocks with infinite resistance. The blocks are connected through a deformable mortar with a finite resistance. This connection is modelled through a sample of points, called *control points*, disposed on the edges of the elements, at which the interaction law depending on the mechanical characteristics and the geometry of the mortar is associated. At each *control point*, also, the portion representative of the contact area between contiguous elements is assigned. An example of the elements representative of the wall is reported in Figure 4.3.1 and the considered modelling in 2D of the wall is represented in Figure 4.3.1, in which different colors have been used to indicate different interaction laws among the elements.

The wall is predominantly constituted by blocks having the same

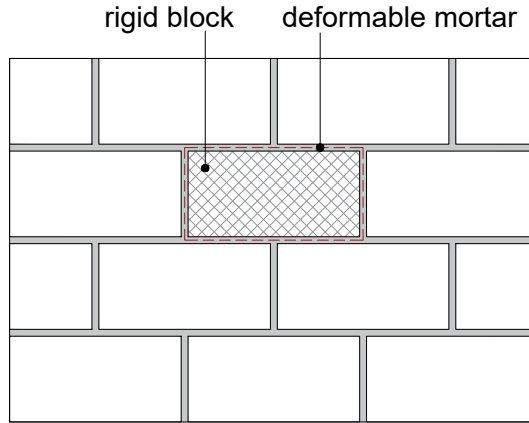


Figure 4.11: The elements constituting the wall

dimensions. However, to ensure the perfect fit of the façade some blocks with an half length are needed on the extremities, as shown in the Figures 4.3.1. On this basis, one or two *control points* are assigned depending on the geometry of the elements. In the first case, the *control point* is located in the centre of the edge, while in the second cases they are located on $1/4$ and $3/4$ of the length of the edge.

The portion representative of the contact area associated to each *control point* depends on the depth of the element and on the number of points on the edge. If one point is associated to the edge, the total length of the block is used to define the contact area; while if two points are associated to the edge, just half of the length of the block is used (Figure 4.3.1).

Both normal and tangential forces act on the contact area, and they depend on the reciprocal displacements of contiguous elements and on the stiffness values of the mortar. With the aim to calculate the

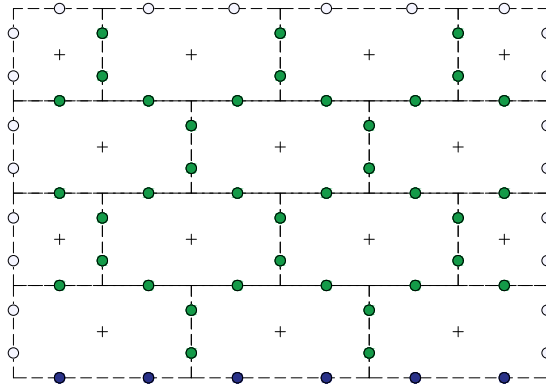


Figure 4.12: The modelling of the wall: the control points

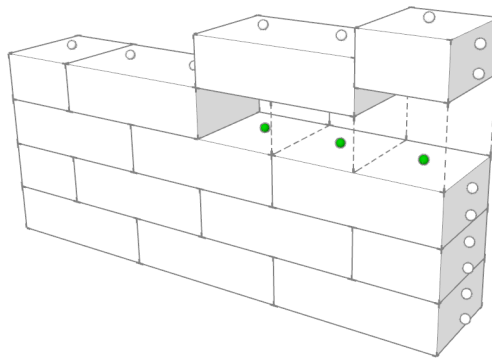


Figure 4.13: The contact areas associated to the control points

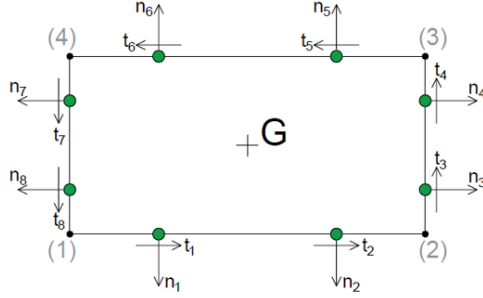


Figure 4.14: Reference Systems associated to the control points of an element

forces components in these areas, a specific reference system with normal and tangential axes has to be associated to each control point and, also, a relationship between two control points belonging to two different elements has to be established. The reference system have been defined so that the normal axis goes outward from the element and the tangential one is rotated counter clockwise in respect to the normal. In Figure 4.3.1 the reference system of the *control points* associated to a single element have been presented. The connection between two (and two only) *control points* is established by the tool on the basis of their global coordinates and on the angle generates by their normal axes. In particular, at each time step the procedure verifies if the distance between two generic contact points of the system and the angle generates by their normal axes are minor of fixed values of tollerance. If this check is satisfied, it means that the considered points are close enough, and their lying are such that the two elements manage to interface. In Figure 4.3.1 an example of check is reported.

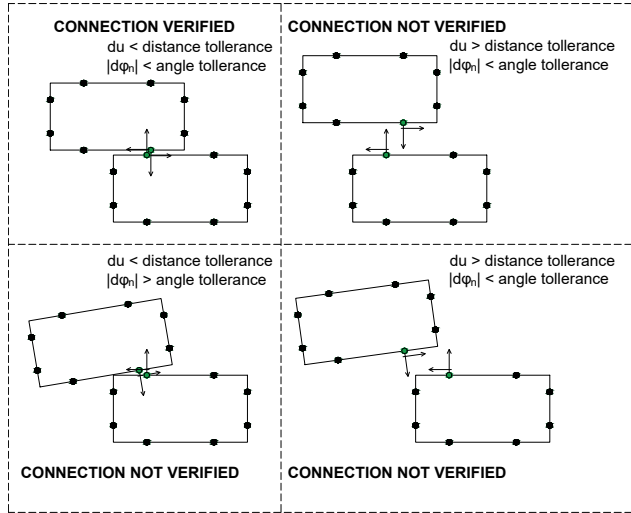


Figure 4.15: Verifying of connection among the control points

4.3.2 The static values in the contact points

At each *control point* of the wall system, one normal and one tangential force is assigned (F_n and F_T respectively) on the basis of the contact law and the relative displacements of the connected *control point*. The interaction between two control points can be governed by an elastic law if there are no cracks in the mortar, or by a frictional law if the crack is verified. The developed procedure always calculates the elastic quantities by the equations 4.8 in which:

- k_{n_i} is the normal stiffness associated to the investigated *control point* i
- k_{t_i} is the tangential stiffness associated to the investigated *control point* i

-
- $d_{n_{ji}}$ is the relative displacement with the connected *control point* j in the direction of the normal axis associated to the investigated *control point* i
 - $d_{t_{ji}}$ is the relative displacement with the connected *control point* j in the direction of the tangential axis associated to the investigated *control point* i

$$\begin{aligned} f_{n_i} &= k_{n_i} \cdot d_{n_{ji}} \\ f_{t_i} &= k_{t_i} \cdot d_{t_{ji}} \end{aligned} \quad (4.8)$$

The equations 4.8 can be written synthetically as in the 4.9. If the crack is verified and field is frictional, the procedure deletes the elastic contributes associating zero values to the stiffnesses parameters k_{n_i} and k_{t_i} where necessary. The frictional contribute is, instead, taked into account through a force vector associated to the element at which the *control point* belongs.

$$f_i = k_i \cdot d_{ji} \quad (4.9)$$

In the following, the model of the mortal behaviour on the basis of the cracks and the evaluation of the relative displacements between two connected *control points* is presented.

The relative displacements between the contact points

The displacements of the *contact point* j in the local system of the *contact point* i can be written on the basis of the global displacements of the points i and j as in the 4.10, according to the quantities reported in Figure 4.3.2

$$\begin{bmatrix} d_{n_{ji}} \\ d_{t_{ji}} \end{bmatrix} = \begin{bmatrix} \cos \phi_{n_i} & \sin \phi_{n_i} \\ -\sin \phi_{n_i} & \cos \phi_{n_i} \end{bmatrix} \cdot \begin{bmatrix} u_j - u_i \\ v_j - v_i \end{bmatrix} \quad (4.10)$$

in which:

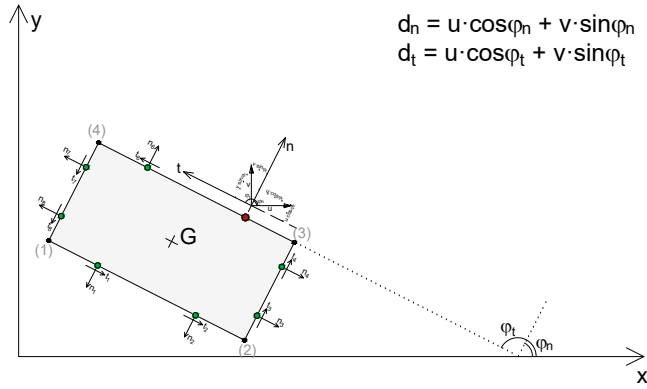


Figure 4.16: Displacements in the local system

- ϕ_{ni} is the angle that the normal axis of the reference system associated to the point i generates with the x axis of the global reference system;
- u_i and v_i are the horizontal and vertical displacements of the point i in the global reference system;
- u_j and v_j are the horizontal and vertical displacements of the point j in the global reference system;

The equation 4.10 can be synthetically written as in the 4.11

$$d_{ji} = \mathbf{R}_i \cdot \Delta u \quad (4.11)$$

in which d_{ji} is the vector of the relative displacements of the point j in the reference system of the point i , \mathbf{R}_i is the rotation matrix and

Δu is the relative displacements between the point j and the point i . Since the elements of the system are rigid, the displacements of an its generic *control point* i belonging to the element e in the global reference system can be written as in the 4.12

$$\begin{bmatrix} u_i \\ v_i \end{bmatrix} = \begin{bmatrix} 1 & 0 & -\Delta y_i \\ 0 & 1 & \Delta x_i \end{bmatrix} \cdot \begin{bmatrix} u_{G_e} \\ v_{G_e} \\ \phi_{G_e} \end{bmatrix} \quad (4.12)$$

in which:

- u_{G_e} is the horizontal displacement associated to the barycenter G of the element e ;
- v_{G_e} is the vertical displacement associated to the barycenter G of the element e ;
- ϕ_{G_e} is the rotation associated to the barycenter G of the element e ;
- Δx_i is the horizontal coordinate of the point i in the baricenter reference system of the element e ;
- Δy_i is the vertical coordinate of the point i in the baricenter reference system of the element e .

The equation 4.12 can be synthetically written as in the 4.13, in which the matrix \mathbf{B}_{e_i} contains the coordinates of the point i in the barycentric reference system of the element e .

$$u_i = \mathbf{B}_{e_i} \cdot u_{G_e} \quad (4.13)$$

At the end, using f to indicate the element at which the point j belongs, the displacements of the point j in the local system of the point i can be written as in the 4.14.

$$d_{ji} = \mathbf{R}_i \cdot (\mathbf{B}_{e_i} \cdot u_{G_e} - \mathbf{B}_{f_j} \cdot u_{G_f}) \quad (4.14)$$

The mortar behaviour

In the initial step of the procedure, all the *control points* of the model are in the elastic field, and at each one of them normal and tangential stiffness values k_n and k_t are associated. Their values are calculated as reported in the equations 4.15 and 4.16 in reference to a generic *control point* i ,

$$k_{n_i} = \frac{E \cdot (b_{p_i} \cdot s_i)}{s_m} \quad (4.15)$$

$$k_{t_i} = \frac{G \cdot (b_{p_i} \cdot s_i)}{s_m} \quad (4.16)$$

in which:

- E is the normal elastic modulus of the mortar;
- G is the tangential elastic modulus of the mortar;
- b_{p_i} is the length of the element associated to the control point i on the considered direction;
- s_i is the depth of the element at which the control point i belongs;
- s_m is the width of the mortar.

When the analysis is processed, the tensile configuration of the contact area in each time step is estimated exploiting the 4.17 and 4.18, in which A_i is the area associated to the *contact point*.

$$\sigma_{n_i} = \frac{f_{n_i}}{A_i} \quad (4.17)$$

$$\sigma_{t_i} = \frac{f_{t_i}}{A_i} \quad (4.18)$$

These values are compared with the limit ones associated to the mortar. In particular, about the normal values the procedure considers an infinite value of compressive resistance $\sigma_{n,sup}$ and a finite value of tensile resistance $\sigma_{n,inf}$ depending on the quality of the mortar. The limit tangential value of mortar is calculated with the Coulomb Law in the 4.19,

$$\sigma_{t,max} = c + \sigma_n \cdot \tan \theta \quad (4.19)$$

in which:

- c is the cohesion of the mortar;
- σ_n is the normal tensile solicitation;
- θ is the attrition angle of the mortar.

If one of the conditions in the 4.20 is true, the crack is verified the law that governs the interaction between the connected *control point* is frictional.

$$\begin{aligned} \sigma_n &< \sigma_{n,inf} \\ |\sigma_t| &> \sigma_{t,max} \end{aligned} \quad (4.20)$$

In this field, another check has to be done to establish the new contact law, i. e. if on the contact surface there is a compressive or a tensile solicitation. In the first case, the interaction between the *contact points* is established yet while in the second case the behaviours of the two faces are independent. The compressive or tensile solicitation is estimated on the basis of the relative displacements of the connected points in the previous step. If a compressive configuration results in the previous step then the normal stiffness value k_n associated to the *control point* is calculated as in the 4.15, while if a tensile configuration results then

Table 4.1: Stiffness values in elastic and frictional fields for the control points

	Elastic Field	Frictional Field
Compressive	$k_n = \frac{E \cdot (b_p \cdot s)}{s_m}$	$k_n = \frac{E \cdot (b_p \cdot s)}{s_m}$
Tensile		$k_n = 0$
Tangential	$k_t = \frac{G \cdot (b_p \cdot s)}{s_m}$	$k_t = 0$ $F_t = \mu \cdot F_n$

stiffness value k_n is considered equal to zero. At the end, the tangential value k_t associated to the point is considered equal to zero, and the tangential force contribute of the *control point* is calculated as in the 4.21, in which μ is the friction coefficient of the material.

$$f_t = \mu \cdot f_n \quad (4.21)$$

It is, obviously obtained that if a tensile solicitation is associated to the point then the normal force F_n is equal to zero and, consequently, the tangential force F_t is null, too.

In the Table 4.1 and Figure 4.3.2 the stiffness values in each possible configuration and the cycle of the check have been summarized.

4.3.3 The stiffness matrix

The stiffness matrix describes the elastic relations among the elements of the wall. In Figure 4.3.3 an example of the composition of a stiffness matrix for the represented six-elements wall is proposed, in which:

- green submatrices \mathbf{K}_{ee} represents the elastic relation of the element with itself;
- light green submatrices \mathbf{K}_{ef} represents the elastic relation that the element i has with the element j ;

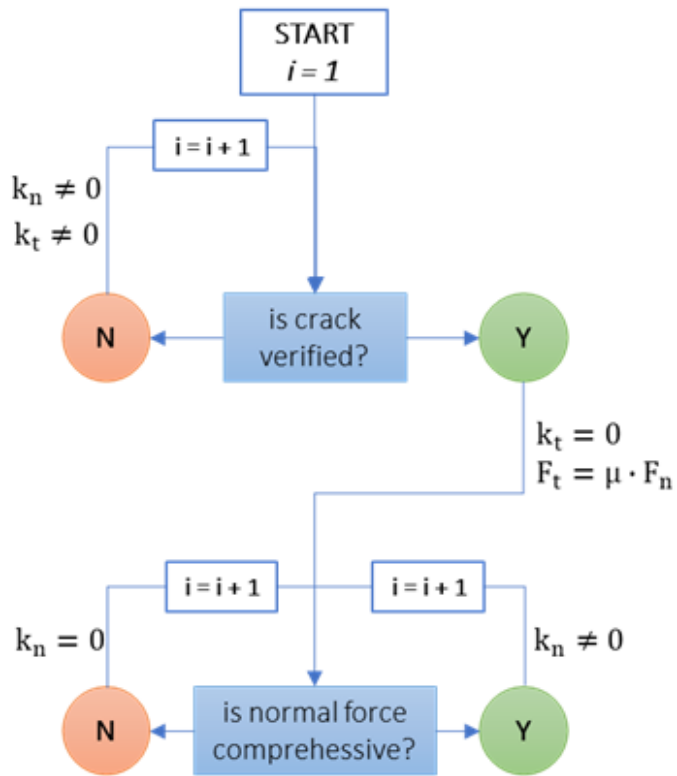


Figure 4.17: Cycle to define the mechanical field of the mortar in the control points

Chapter 4. Seismic behaviour of masonry buildings, out of plane and in plane, through limit state and D.E.M. analyses

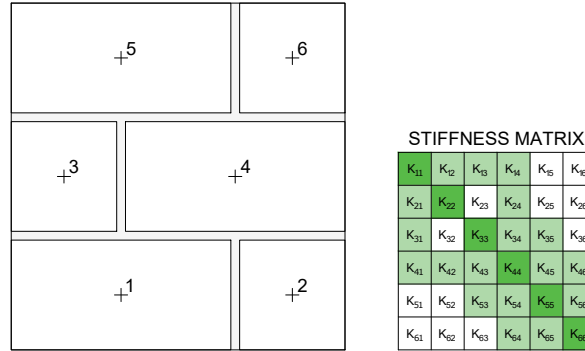


Figure 4.18: Example of the composition of the stiffness matrix

- white submatrices \mathbf{K}_{ef} , constituted by all elements equal to zero, represents the no relation between the element i with the element j .

Furthermore, the stiffness matrix represents the relation between the vector \mathbf{F} representative of the elastic forces F_{G_x} , F_{G_y} and M_{G_z} applied in the baricenter of the elements, and the vector \mathbf{d} representative of the displacements u_G , v_G and ϕ_G of the baricenter of the elements.

In the procedure the stiffness submatrix relative to each single element of the wall (Figure 4.3.3) is estimated and, at the end, the global stiffness matrix is assembled.

The stiffness submatrices of each element have been defined through a condition of elastic equilibrium. Set e to indicate the analysed element and F to indicate the generic element to e through *control points*. Set, also i and j to indicate the connected *control points* of

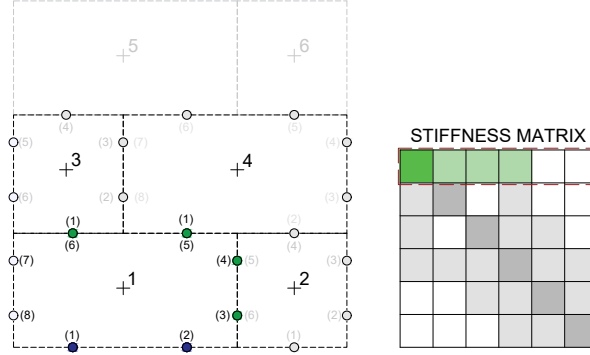


Figure 4.19: Example of the composition of the submatrix of the element 1

the elements e and f respectively. Exploiting the equations 4.11, 4.15 and 4.16 the normal and tangential components of the elastic forces assigned in each *control point* i of the analyzed element e through the 4.9. As shown in Figure 4.3.3, the local forces f_i can be written in the global reference system as in the 4.22.

$$F_i = \mathbf{R}_i^T \cdot f_{e_i} \quad (4.22)$$

in which F_i are the components of the force assigned to the point i in the global reference system and \mathbf{R} is the rotation matrix introduced in the equation 4.11.

Using F_{G_e} to indicate the forces applied in the baricenter of the element e , the equilibrium condition of the element in respect to its baricenter can be written as in the 4.23

$$F_{G_e} = \mathbf{B}_e^T \cdot F_{e_i} \quad (4.23)$$

Chapter 4. Seismic behaviour of masonry buildings, out of plane and in plane, through limit state and D.E.M. analyses

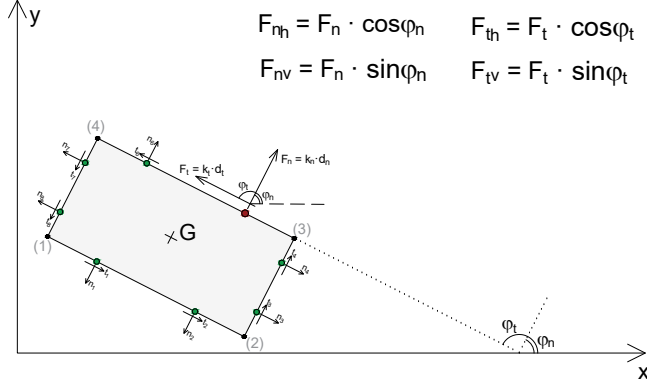


Figure 4.20: Example of the composition of the stiffness matrix

in which B_e^T is the transposed of assembled matrix \mathbf{B}_e of the submatrices \mathbf{B}_{e_i} introduced into the 4.13. At the end, substituting the 4.11, 4.15 and 4.16 the 4.24 is obtained.

$$F_{G_e} = \mathbf{B}_e^T \cdot \mathbf{R}_e^T \cdot k_e \cdot \mathbf{R}_e \cdot (\mathbf{B}_e \cdot u_{G_e} - \mathbf{B}_f \cdot u_{G_f}) \quad (4.24)$$

From the 4.24, the submatrices of the element e can be obtained as in the 4.25 and 4.26.

$$K_{ee} = \mathbf{B}_e^T \cdot \mathbf{R}_e^T \cdot k_e \cdot \mathbf{R}_e \cdot \mathbf{B}_e \quad (4.25)$$

$$K_{ef} = -\mathbf{B}_e^T \cdot \mathbf{R}_e^T \cdot k_e \cdot \mathbf{R}_e \cdot \mathbf{B}_f \quad (4.26)$$

4.3.4 The mass matrix

The mass matrix is obtained assembling the mass submatrices associated to each element of the system. The mass is a specific quantity associated at each element, and it does not generate relations with the other blocks. For this reasons, the submatrices \mathbf{M}_{ef} representatives of the mass relation between the generic elements e and f is null. The submatrix \mathbf{M}_{ee} , instead, depends on the mass m_e of the element e , calculated as in the 4.27,

$$m_e = \gamma_e \cdot b_e \cdot h_e \cdot s_e \quad (4.27)$$

in which:

- γ_e is the relative density of the element e ;
- b_e is the length of the element e ;
- h_e is the height of the element e ;
- s_e is the depth of the element e .

The submatrix M_{ee} associated to the element e is obtained as in the 4.28,

$$\mathbf{M}_{ee} = \begin{bmatrix} 1 & 0 & 0 \\ 0 & 1 & 0 \\ 0 & 0 & \rho_{e,xy}^2 \end{bmatrix} \cdot m \quad (4.28)$$

in which ρ_e is the radius of the polar gyration of the element e in the plane xy .

4.3.5 The damping matrix

Whit the aim to avoid resonance problems in the model, a damping matrix has been introduced, that contents the velocity components

in acceptable range.

The values of the used damping matrix has been considered as percentage of the critic damping C_C calculated in the 4.29

$$C_C = 2 \sqrt{K^{-1} M} \quad (4.29)$$

in which K and M are the stiffness matrix and the mass matrix respectively.

The damping matrix C considered in the procedure is the 5% of the critic one, as reported in the 4.30.

$$C = 0.05 \cdot C_C \quad (4.30)$$

4.3.6 The Newmark method

The Newmark Method belongs to the family of the methods to finite differences. This model provides for the discretization of the time interval of analysis in fixed time steps Δt . In particular, knowing the configuration of the system at the initial instants, this method evaluates the solution at the subsequent time step. This solution becomes the initial condition for the next calculation step. The balance problem is governed by the generic equation given in the 4.31.

$$M\ddot{u}(t) + C\dot{u}(t) + Ku(t) = F(t) \quad (4.31)$$

in which:

- M is the mass matrix of the system;
- C is the damping matrix of the system;
- K is the stiffness matrix of the system;
- $\ddot{u}(t)$ is the acceleration vector of the system in the instant t ;

-
- $\dot{u}(t)$ is the velocity vector of the system in the instant t ;
 - $u(t)$ is the displacement vector of the system in the instant t ;
 - $F(t)$ is the external forces vector applied to the system in the instant t ;

The unknowns of the problem are the kinematic variables. Exploiting the Lagrange method, the relations among these variables can be expressed. In particular, using j to indicate the generic time step, velocity and displacement can be written as in the 4.32 and 4.33 respectively.

$$\dot{u}_{j+1} = \dot{u}_j + \Delta t [(1 - \gamma) \ddot{u}_j + \gamma \ddot{u}_{j+1}] \quad (4.32)$$

$$u_{j+1} = u_j + \Delta t \dot{u}_j + 0.5 \cdot \Delta t^2 [(1 - 2\beta) \ddot{u}_j + 2\beta \ddot{u}_{j+1}] \quad (4.33)$$

where Δt is the time step.

Replacing the 4.32 and 4.33 in the 4.31 the 4.34 is obtained, an equation in which the only unknown is the \ddot{u}_{j+1} .

$$\begin{aligned} &\mathbf{M}\ddot{u}_{j+1} + \mathbf{C}\{\dot{u}_j + \Delta t[(1 - \gamma)\ddot{u}_j + \gamma\ddot{u}_{j+1}]\} + \\ &+ \mathbf{K}\{u_j + \Delta t\dot{u}_j + 0.5\Delta t[(1 - 2\beta)\ddot{u}_j + 2\beta\ddot{u}_{j+1}]\} = F(t) \end{aligned} \quad (4.34)$$

Introducing the quantities \mathbf{M}^* and F^* like as in the 4.35 and 4.36 respectively, the \ddot{u}_{j+1} can be estimated as in the 4.37.

$$\mathbf{M}^* = \mathbf{M} + \mathbf{C}\Delta t\gamma + \mathbf{K}\Delta t^2\beta \quad (4.35)$$

$$\begin{aligned} F^* = F_{j+1} + &(\mathbf{C}\Delta t\gamma + \mathbf{K}\Delta t^2\beta - \mathbf{C}\Delta t - 0.5\mathbf{K}\Delta t^2)\ddot{u}_j \\ &-(\mathbf{C} + \mathbf{K}\Delta t)\dot{u}_j - \mathbf{K}u_j \end{aligned} \quad (4.36)$$

$$\ddot{u}_{j+1} = \frac{\mathbf{F}^*}{\mathbf{M}^*} \quad (4.37)$$

At the end, the \ddot{u}_{j+1} can be replaced in the 4.32 and 4.33 so that the kinematic configuration of the system can be known.

4.3.7 The time step

The definition of the time step depends on the natural period of the elements of the system. The equation of motion of a linear system with multiple degree of freedom, not damped and with a free vibration assumes the form in the 4.38.

$$\mathbf{M}\ddot{\mathbf{u}}(t) + \mathbf{K}\mathbf{u}(t) = \mathbf{0} \quad (4.38)$$

where $\mathbf{0}$ is a vector with all-zero components. Exploiting the analogy with the behaviour of a system with a single degree of freedom, it is assumed that the motion in free vibration is harmonic and assumes the form reported in the 4.39.

$$\mathbf{u}(t) = \bar{\mathbf{u}} \cdot \sin(\omega t + \theta) \quad (4.39)$$

in which $\bar{\mathbf{u}}$ is a vector that does not depend on time and represents the shape of the configuration of the system during the cycle. The amplitude of this shape varies over time according to the function $\sin(\omega t + \theta)$ and θ is the phase angle. Deriving twice the 4.39 it is obtained the 4.40.

$$\ddot{\mathbf{u}}(t) = -\omega^2 \cdot \bar{\mathbf{u}} \cdot \sin(\omega t + \theta^*) \quad (4.40)$$

The system always admits the trivial solution $\bar{\mathbf{u}} = \mathbf{0}$ that corresponds to the configuration in which the system is motionless. The

non-trivial solutions, that corresponds to the possible configurations of dynamic balance, is obtained when the 4.41 is verified.

$$(\mathbf{K} - \omega^2 \mathbf{M}) = 0 \quad (4.41)$$

The values of ω that gives the solution of the problems are given by the 4.42.

$$\omega^2 = \sqrt{\mathbf{M}^{-1} \mathbf{K}} \quad (4.42)$$

that are the natural frequencies of each element of the wall. Keeping in mind the relation between the natural period and the natural frequency, the time step in the procedure is taken as the smaller of the all natural periods of the system, calculated as in the 4.43.

$$\Delta t = \frac{2\pi}{\max(\omega)} \quad (4.43)$$

4.3.8 The achievement of the levels of damage

The dynamic analysis of the model can define the geometrical wall configuration, the tensile field and the crack pattern in each considered time step. The definition of the level of damage of the building used in this work is based on kinematic aspects, and it takes into account the dislocations and the frictional field in the considered wall.

It's important to keep in mind that analyses study the structural part of the building, so that the level of damage D1, that refers to the not structural damage, can't be efficiently estimated. Furthermore, analytically it can be difficult to distinguish the partial collapse of the building (D4) to the total one (D5). For these reasons, only the vulnerability curves in reference to the levels of damage D2, D3 and D4 are calculated.

Specifically, the adopted limit values are:

- D2 is reached 30% of the contact points are in frictional field;
- D3 is reached the first time that two elements are distant more than 2 mm;
- D4 is reached the first time that two elements are distant more than $1/4$ of the basis of the elements.

4.4 The vulnerability factors

The vulnerability factors considered in the model can be classified in three typologies: material modifier, geometrical modifier and typological modifier. In the first group there are the mechanical characteristics of the mortar. In particular, the parameters that must be defined are:

- E , the elastic modulus of the mortar;
- ν , the Poisson modulus of the mortar;
- c , the cohesion of the mortar;
- ϕ , the attritive angle of the mortar;
- $\sigma_{n,inf}$ the limit value of traction of the mortar.

In the second group there are the geometrical parameters of the elements and mortar, and the dimension of the wall and opening. In particular:

- b , the length of the element;
- h , the height of the element;

-
- s , the depth of the element;
 - s_m , the thickness of the mortar;
 - B , the base of the wall;
 - H_i , the height of a single storey;
 - B_w , the base of the windows;
 - H_w , the height of the windows.

In the third group there are the typological characteristics of the masonry buildings. In particular, the considered modifiers have been:

- the number of floors (Figure 4.4);
- the type of horizontal structure (Figure 4.4);
- the horizontal connections (Figure 4.4);
- the number and the position of the openings (Figure 4.4).

Number of floors

The number of floors is the easier parameter to insert in the model because it's enough to insert another brick row covering a further inter-storey. Although it is particularly easy to model this type of parameter, it should be noted that the number of plans is one of the parameters that most affects the computational burden of the model. Consider, for example, that the basic dimensions and height of a blind facade and the dimensions of the block are fixed.

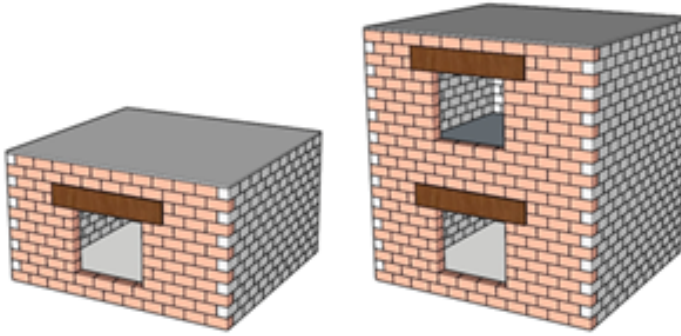


Figure 4.21: Vulnerability factor: number of floors

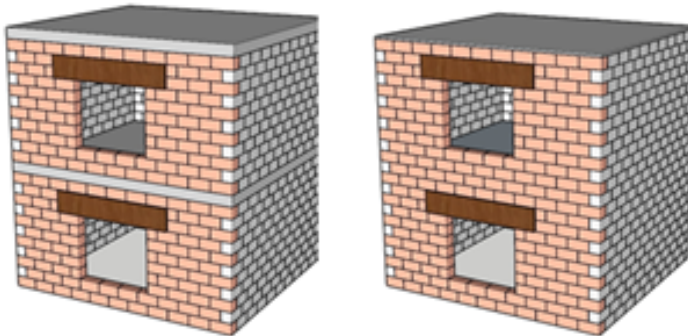


Figure 4.22: Vulnerability factor: horizontal structure

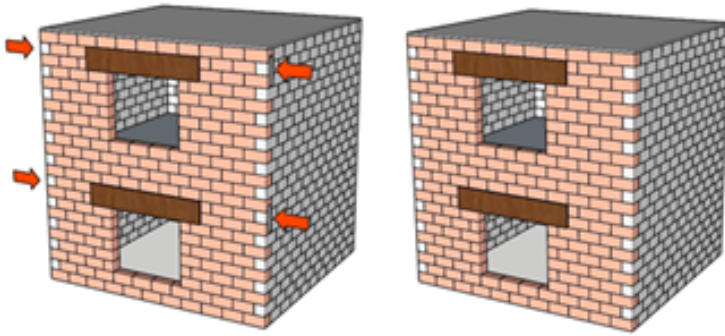


Figure 4.23: Vulnerability factor: horizontal connections

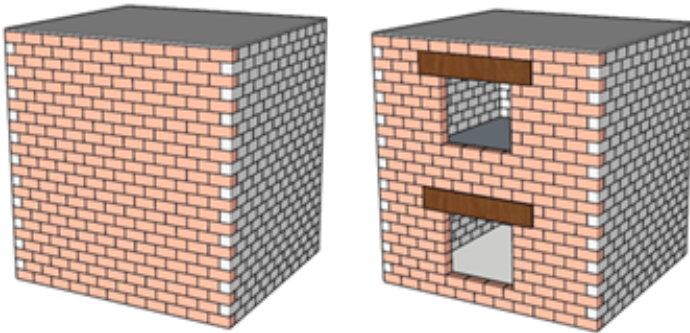


Figure 4.24: Vulnerability factor: openings

If you increase the number of planes from one to two, the number of elements to be considered in the modelling doubles, and the stiffness, mass and damping matrices quadruple the number of elements. For this reason, the variability of the parameter is restricted on the choice of 1 or, maximum, 2 floors, also according to the sample reference for the C class.

Horizontal structure

The horizontal structure of the masonry building can be considered rigid, if it's realized in a concrete or steel material, or deformable, if is realized in wood. In the first case, in the summit of each rows of brick covering an inter-storey, another rigid block having the length of the wall and the height of 0.30 m is insert, and all the control points of the elements strictly above and below are connected to this rigid block. The weight of the floor is associated to the rigid block.

If the horizontal structure is considered as deformable, there are no rigid block insert in the wall, and the weight of the floor is associated to the last row of element that covers the inter-storey.

Horizontal connections

The horizontal connections are technological solutions often adopted when the horizontal structure is not rigid. The variability of this parameter is, for this reason, considered only when a deformable horizontal structure is chosen in the model. In particular, if horizontal connections are taken into account comprehensive solicitations are applied on the external bricks of the last row of elements of each storey.

Openings

In the model is considered that each storey can have zero, one or two windows. The insertion of the windows also requires introducing a lintel on the opening. Its dimensions are defined adding 0.30 m to the length of the window in horizontal, and it is of 0.30 m in the vertical dimension.

Chapter 4. Seismic behaviour of masonry buildings, out of plane
and in plane, through limit state and D.E.M. analyses

Chapter 5

Simulations and outcomes

The in plane and out of plane behaviour of the façades have been investigated through the proposed methodologies for a sample of masonry walls built *ad hoc*. In particular, four vulnerability modifiers have been taken into account (number of floors, horizontal structures, ties and openings) and for each of them two classes of variability have been considered. The uniform combination of the class of parameters has been considered, and the sample of $2^4 = 16$ buildings reported in the Table 5.1 has been obtained. For each building of the sample the models for the out of plane and in plane analyses have been adopted, and the PGA values that active the out of plane kinematisms and the in plane levels of damages have been estimated. The outcomes have been summarized in the Tables 5.1 and 5.2 for the in plane and out of plane analyses respectively.

On the basis of these accelerations, the vulnerability curves related to each phenomena have been built. On the basis of the assumption of uniform distribution of the walls in the sample, a probability of occurrence equal to $1/16$ has been assigned to each façade and the vulnerability curves have been built as in the equation 3.2. In

Table 5.1: PGA values for the achievement of the in plane levels of damage for each building of the sample

floors	horizontal structure	ties	openings	PGA_{D2}	PGA_{D3}	PGA_{D4}
1	deformable	yes	0	0.31	0.58	0.63
1	deformable	yes	2	0.17	0.27	0.48
1	deformable	no	0	0.06	0.14	0.26
1	deformable	no	2	0.05	0.10	0.23
1	rigid	yes	0	0.45	0.61	0.68
1	rigid	yes	2	0.32	0.41	0.57
1	rigid	no	0	0.30	0.38	0.56
1	rigid	no	2	0.17	0.27	0.50
2	deformable	yes	0	0.12	0.16	0.38
2	deformable	yes	2	0.08	0.16	0.38
2	deformable	no	0	0.02	0.09	0.16
2	deformable	no	2	0.02	0.08	0.14
2	rigid	yes	0	0.16	0.22	0.47
2	rigid	yes	2	0.15	0.22	0.40
2	rigid	no	0	0.07	0.15	0.31
2	rigid	no	2	0.10	0.16	0.33

Table 5.2: PGA values for the achievement of the out of plane mechanism for each building of the sample

floors	horizontal structure	ties	openings	$PGA_{s.o.}$	$PGA_{v.b.}$	$PGA_{h.b.}$
1	deformable	yes	0	0.95	2.22	0.77
1	deformable	yes	2	0.85	2.00	0.62
1	deformable	no	0	0.33	2.22	0.77
1	deformable	no	2	0.30	2.00	0.62
1	rigid	yes	0	1.03	2.80	0.75
1	rigid	yes	2	0.93	2.52	0.60
1	rigid	no	0	0.42	2.80	0.75
1	rigid	no	2	0.37	2.52	0.60
2	deformable	yes	0	0.49	0.48	0.77
2	deformable	yes	2	0.44	0.43	0.62
2	deformable	no	0	0.07	0.27	0.77
2	deformable	no	2	0.06	0.25	0.62
2	rigid	yes	0	0.52	0.48	0.75
2	rigid	yes	2	0.46	0.44	0.60
2	rigid	no	0	0.09	0.29	0.75
2	rigid	no	2	0.08	0.26	0.60

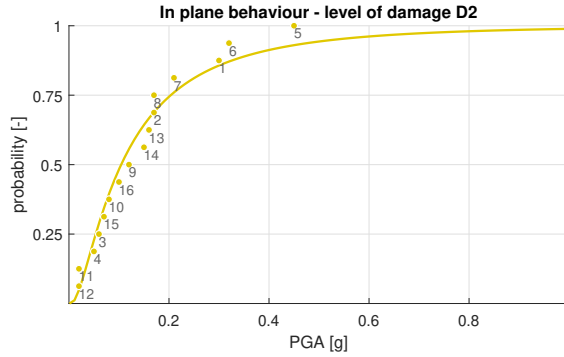


Figure 5.1: Vulnerability curve D2 for the in plane analysis in reference to the considered sample

Figures 5.1 - 5.6 the outcomes have been reported. The vulnerability curves obtained for the in plane behaviour, representative of the levels of damage D2, D3 and D4 (Figure 5.1 - 5.2 - 5.3 respectively) show a perfect correspondence of building typologies on the PGA values. With reference to the out of plane analyses, the vulnerability curve of the simple overturning phenomena (5.4) shows the high standard deviation of the function, contrary to the vulnerability curve of the horizontal bending (Figure 5.6) for which the sample shows a little variation. The vulnerability curve of the vertical bending phenomena (Figure 5.5) is in the middle. The reasons about the variability of these curves can be found in the Section 4.2, in which the equation for the evaluation of the collapse multiplier of the three collapse mechanisms have been reported. It is shown that the equation for the evaluation of the horizontal bending does not depends on ties and number of floors but just on the static

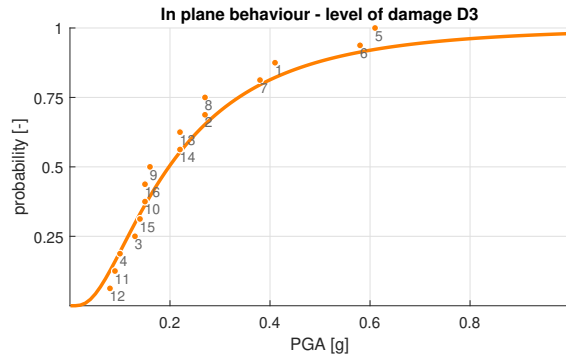


Figure 5.2: Vulnerability curve D3 for the in plane analysis in reference to the considered sample

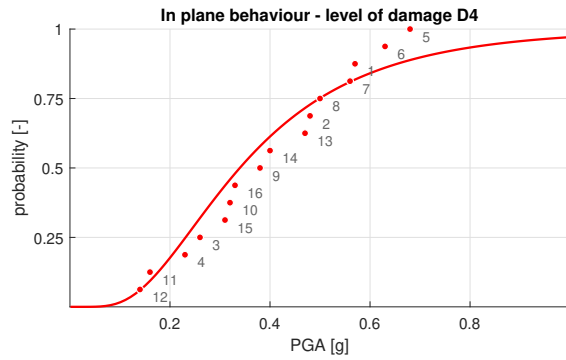


Figure 5.3: Vulnerability curve D4 for the in plane analysis in reference to the considered sample

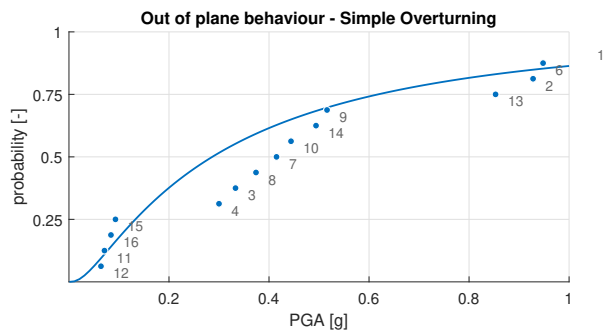


Figure 5.4: Vulnerability curve of simple overturning in reference to the considered sample

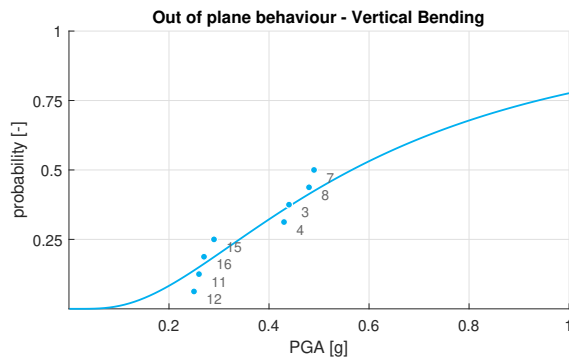


Figure 5.5: Vulnerability curve of vertical bending in reference to the considered sample

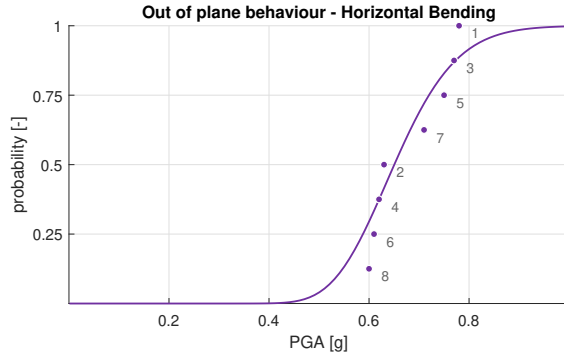


Figure 5.6: Vulnerability curve of horizontal bending in reference to the considered sample

and geometric quantities. The openings and horizontal structures just light change the static values of the loads and consequently the variability of behaviour of the building in the sample is contained in reference to the horizontal bending. On the other hand, the simple overturning depends on all the four considered parameters, so that the variability of behaviour for the buildings in the sample is high, consequently, its dispersion on the PGA. The equations of the vertical bending show that if the building has one floor there is no dependence of the phenomena by the ties, contrary to the case in which the building has two floors. The buildings distribution on the PGA values for the vertical bending is high influenced by the floor of the buildings. In Figure 5.7 both the in plane curves than the out of plane curves have been represented. It is shown that the vertical and the horizontal bending always occur after the achievement of the level of damage D4 in the plane. The simple overturning, in-

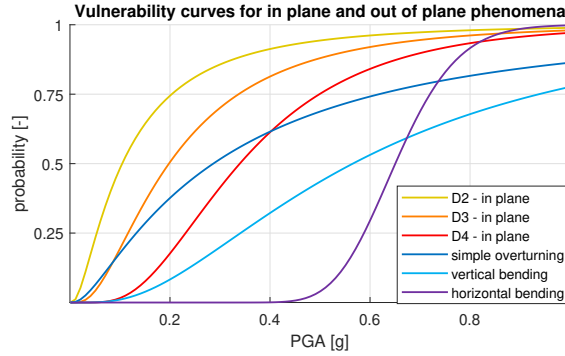


Figure 5.7: Vulnerability curves of in plane and out of plane phenomena

stead, has a behaviour similar to the level of damage D3 in plane for low values of PGA and overcomes the level of damage D4 in plane for high values of PGA. It has to be considered that for buildings without ties the box effect is not verified so the behaviour of the orthogonal walls is independent. For this reason in this cases it is reasonable that the overturning of a façade occurs before than the orthogonal wall reaches a level of damage equal to D4.

In Figures 5.8 - 5.11 the influence of the number of floors have been represented for the in plane levels of damage D3 -D4 and the out of plane mechanisms of simple overturning and vertical bending respectively. At the same way, in Figures 5.12 - 5.15 the influence of the ties have been represented. It has to be highlighted that the representation of the influence of the ties for the vertical bending has been expressed for buildings with two floors only since for buildings of one floor there is not the influence of the ties. The level of

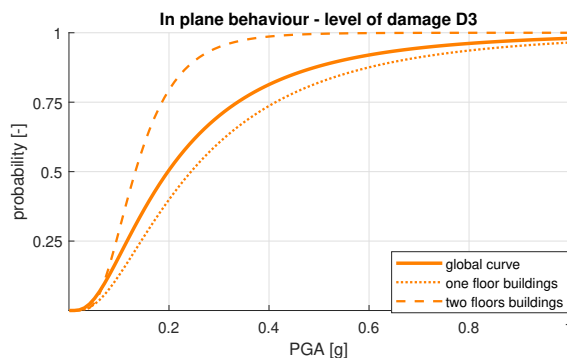


Figure 5.8: Vulnerability curve D3 for the in plane analysis with reference to the influence of the number of floors

damage D2 difference for floors has not been represented since its low interest on the definition of significant structural damage and, on the other hand, the horizontal bending has not been represented since its no dependence by the considered parameters.

The Figures show that both for the in plane behaviour that the out of plane behaviour, the buildings distribution on the PGA values is more influenced by the presence of ties than for the number of floors, except for the vertical bending. Furthermore, the influence of both parameter is more significant for the out of plane behaviour that for the in plane one. It corresponds to the concept that the high inertia of a façade in its plane guarantees a better and more predictable behavior in respect to its section, for which the inertia is very low.

A study has, also, been focused on the influence of the ties on the simple overturning for the box effect. In Figures 5.16 - 5.17

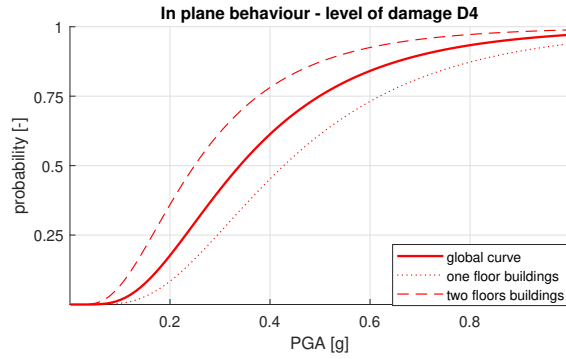


Figure 5.9: Vulnerability curve D4 for the in plane analysis with reference to the influence of the number of floors

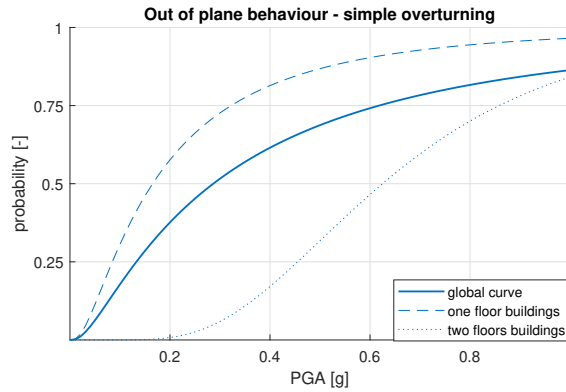


Figure 5.10: Vulnerability curve of simple overturning with reference to the influence of the number of floors

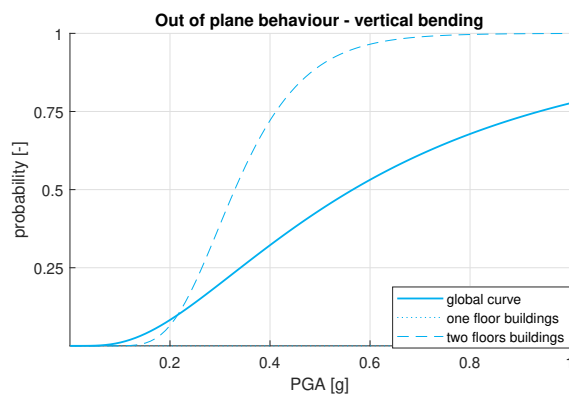


Figure 5.11: Vulnerability curve of vertical bending with reference to the influence of the number of floors

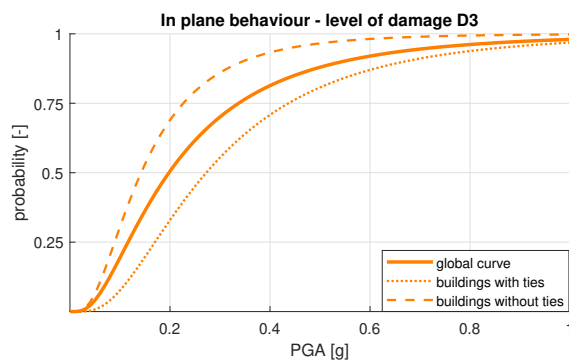


Figure 5.12: Vulnerability curve D3 for the in plane analysis with reference to the influence of the ties

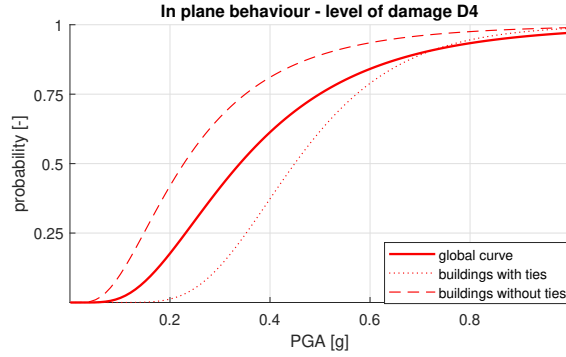


Figure 5.13: Vulnerability curve D4 for the in plane analysis with reference to the influence of the ties

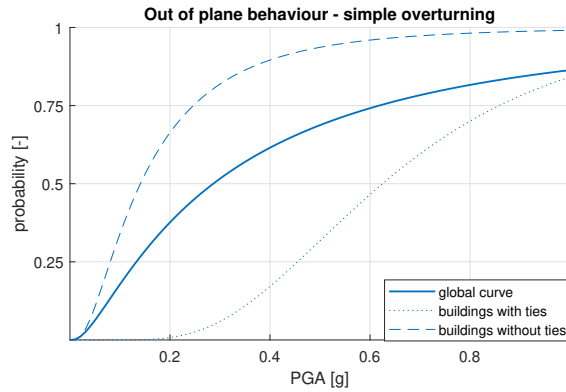


Figure 5.14: Vulnerability curve of simple overturning with reference to the influence of the ties

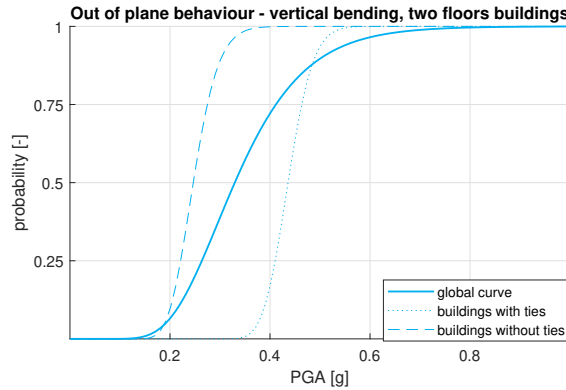


Figure 5.15: Vulnerability curve of vertical bending with reference to the influence of the ties

have been represented the in plane behaviour on th three degree of damage and the simple overturning for buildings without ties and buildings with ties respectively. In Figure 5.16 is evident the independence of the walls: in fact the overturning of the façade occurs in correspondence of the level of damage D3 in plane. Figure 5.17, instead, shows that the simple overturning of a façade for buildings with ties always occurs after the achievement of the level of damage D4 in plane. At the end, in Figure 5.18 has been represented a comparison between the curve representative of the simple overturning for buildings without ties and the curve obtained by the difference between the simple overturning and the D4 in plane for buildings with ties (the green area in Figure 5.17). The discrete element method adopted in the analytical approach has been shown to be able to evaluate with a good approximation the contribution of the orthogonal walls in a box like effect by considerably incre-

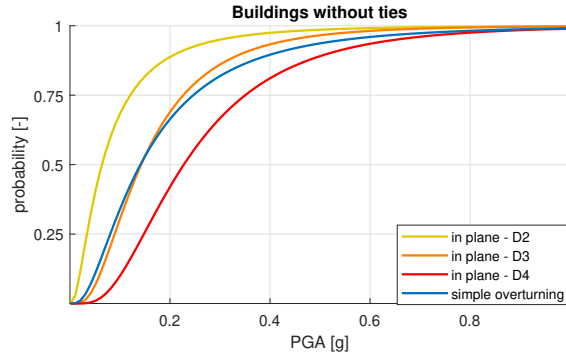


Figure 5.16: Vulnerability curve of vertical bending with reference to the influence of the ties

menting the actions (a_g) for the simple overturning phenomena, responsible of the final collapse of the building.

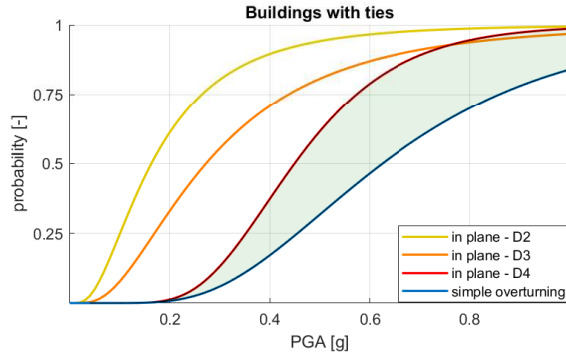


Figure 5.17: Vulnerability curve of vertical bending with reference to the influence of the ties

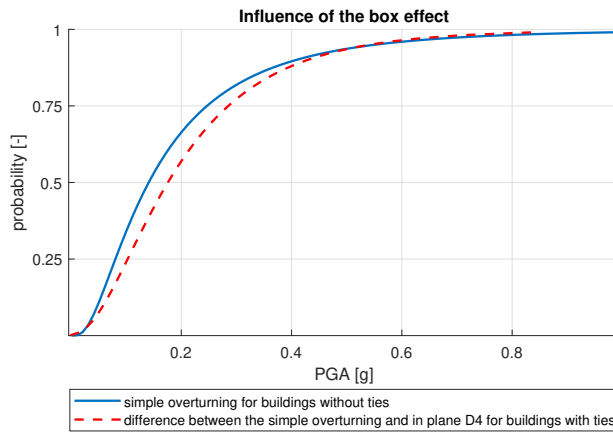


Figure 5.18: Vulnerability curve of vertical bending with reference to the influence of the ties

Conclusions

The work presented in this thesis has the aim to furnish a tool able to define vulnerability curves that describe the behaviour of the Italian masonry buildings.

The work proposes two methodologies to assess the seismic vulnerability: one is empirical/observational and the second is analytic. The observational method presented exploits data provided by the PLINIVS Study Center obtained by the surveys activities on buildings damaged by the main Italian seismic events. On the basis of these data a statistical correlations among the most common and influencing typological characteristics of the Italian masonry constructions, the reached damages and the seismic input values has been defined. On these data, the vulnerability curves representative approximately of the whole typologies on the national territory have been built.

The second part of the work defines an analytic tool to define the behaviour of the in plane and out of plane walls of the good quality masonry buildings. The out of plane behaviour of the walls has been investigated on the basis of the kinematic theorem of the limit analysis, that define the conditions of collapse. The in plane behaviour of the walls has been analyzed through a discrete element method with rigid blocks, representative of the good quality bricks, disposed regular and connected with deformable mortar.

For the analytic analysis a virtual sample has been built considering a uniform distribution of buildings types. These buildings types has been defined on the combination of four considered typological characteristics: number of floors, kind of floors, ties and openings. On the basis of this sample the vulnerability curves for the in plane and out of plane behaviour have been built and some comparisons of the outcomes have been presented.

The outcomes shows that:

- The critical approach on empirical procedures to evaluate the vulnerability curves provides scenario very close to detected data.
- The analytical approach produces vulnerability curves not always in line with curves obtained by empirical approach since the second one includes several type of different masonry manufactures.
- The vulnerability modifier that more influences the global behaviour of the building under seismic action is the presence of ties, that contributes considerably to the box-like effect.
- The discrete element method adopted in the analytical approach, on the other hand, has been shown to be able to evaluate with a good approximation the contribution of the orthogonal walls in a box like effect by considerably incrementing the actions (a_g) for the simple overturning phenomena, responsible of the final collapse of the building.

Considering the obtained outcomes, some new purposes can be developed. In particular, on the basis of typological database of the

Italian masonry typologies it could be interesting, and useful, to develop specific vulnerability curves with the analytical procedure at regional scale.

Bibliography

- [1] Borzi, B., Faravelli, M., Onida, M., Polli, D., Quaroni, D., Pagano, M., Di Meo, A. Piattaforma IRMA (Italian Risk MAP) GNGTS: pp382-388 (2018)
- [2] Nicola Cavalieri San Bertolo. Istituzioni di architettura, statica e idraulica Mantova, F.lli Negretti, (1845)
- [3] Alberto Gabba. Corso di costruzioni civili e militari di Alberto Gabba Torino (1876)
- [4] Giovanni Curioni. L'arte di fabbricare, ossia Corso completo di istituzioni teorico-pratiche per gli Ingegneri, per Periti in Costruzione e per Periti Misuratori. six Vol. (1864-1884)
- [5] Giuseppe Campanella. Trattato generale teorico pratico dell'arte dell'ingegnere civile, industriale ed architetto Ed Vallardi - Milano (1928)
- [6] Binda, L., Mirabella, G., Tiraboschi, C., Abbaneo, S. Measuring masonry material properties Proceedings Italian-US Workshop 'Guidelines for Seismic Evaluation and Rehabilitation of Unreinforced Masonry Buildings', NCEER-94-0021, Buffalo NY, pp.6,3-24, (1994)

- [7] Como, M. Equilibrium and collapse analysis of masonry bodies. *Mechanica*, pp184-194 (1992)
- [8] Cundall, P.A. A Computer Model for Simulating Progressive Large Scale Movements in Blocky Rock Systems. *Proceedings of the Symposium of the International Society for Rock Mechanics, Society for Rock Mechanics (ISRM), France, II-8* (1971)
- [9] Cundall, P.A. UDEC - a generalized distinct element program for modeling jointed rock.
- [10] Cundall, P.A. Formulation of a three dimensional distinct element model - Part I: a scheme to detect and represent contacts in a system composed of many polyhedral blocks. *Int J Rock Mech Min Sci Geomech*, pp 107-116 (1988)
- [11] Taylor, L. M. BLOCKS: a block motion code for geomechanics studies. (1983)
- [12] Williams, J. R. The theoretical basis of the discrete element method *Numerical methods in Engineering, theory and application* (1985)
- [13] Williams, J. R., Mustoe, G. W. Modal methods for the analysis of a discrete system *Computational Geotechnique* (1987)
- [14] Cundall, P.A. Numerical modelling of discontinua (1992)
- [15] Heyman, J. The stone skeleton *Journal of solid and structures*, pp. 269-279 (1966)
- [16] Heyman, J. The safety of masonry arches *Journal of mechanic sciences*, pp. 363 - 384 (1969)

-
- [17] Addessi, D., Marfia, S. Sacco, E., Toti, J. Modelling approaches for masonry structures The open civil engineering journal, pp. 288-300 (2017)
- [18] Angelillo, M. Mechanics of masonry structures Vienna, Springer (2014)
- [19] Baratta, A. Statics and reliability of masonry structures General principles application in mechanics and solids and structures CISM, pp 205-235 (1991)
- [20] Del Piero, G. Constitutive equation and compatibility of the external loads for linear elastic masonry-like materials *Mechanica*, pp. 150-162 (1989)
- [21] Di Pasquale, S. Questioni concernenti la meccanica dei mezzi non reagenti a trazione. Unilateral problems in structural analysis, pp. 25-46 (1984)
- [22] Whitman, R. V., Hong, S. T., Reed, J. W. "Damage statistics for high-rise buildings in the vicinity of the San Fernando Earthquake" Department of Civil Engineering Research Report R73-24, M.I.T., April (1973)
- [23] Whitman, R. V., Reed, J. W., Hong, S. T. "Earthquake Damage Probability Matrices" Proceedings of the Fifth World Conference on Earthquake Engineering: pp2531-2540, Rome (1973)
- [24] Braga, F., Dolce, M., Liberatore, D. Southern Italy November 23, 1980 Earthquake: a statistical study of damaged buildings and an ensuing review of the MSK-76 nscale. CNR-PFG (1982)

- [25] Braga, F., Dolce, M., Liberatore, D. Assessment of the relationships between macroseismic intensity, type of buildings and damage, based on the recent Italy earthquake data. European Conference on Earthquake Engineering (1986)
- [26] Benedetti, D., Benzoni, G., Parisi, M. A. Seismic vulnerability risk evaluation for old urban nuclei Earthquake engineering and structural dynamics, pp. 183-201 (1988)
- [27] Riuscetti, M., Carniel, R., Cecotti, C. Seismic vulnerability assessment of masonry buildings in a region of moderate seismicity Analisi di geofisica (1997)
- [28] Colombi, M., Borzi, B., Crowley, H., Onida, M., Meroni, F., Pinho, R. Deriving vulnerability curves using Italian earthquake data Bullet Earthquake Engineering, pp. 485-504 (2008)
- [29] Bernardini, A., Giovinazzi, S., Lagomarsino, S. Vulnerability and prediction of damage at regional scale using a methodology consistent with the EMS-98 macroseismic scale. Convegno ANIDIS (2007)
- [30] Bernardini, A., Giovinazzi, S., Lagomarsino, S. Damage probability matrices implicit in scale EMS 98 by housing typologies. Convegno ANIDIS (2007)
- [31] D'Ayala, D., Speranza, E. Definition of collapse mechanisms and seismic vulnerability of historic masonry buildings. Earthquake spectra, Volume 19, n0. 3, pp 479-509 (2003)
- [32] Valluzzi, M. R., Cardani, G., Binda, L., Modena, C. Seismic vulnerability methods for masonry buildings in historical centres: validation and application for prediction analyses

and intervention proposal. 13^o world conference on earthquake engineering (2004)

- [33] Pasticier, L., Amadio, C., Fragiacomio, M. Non-linear seismic analysis and vulnerability evaluation of a masonry buildings by means of the SAP2000 V.10 code. Earthquake engineering and structural dynamics, pp 467-485 (2007)
- [34] Borzi, B., Crowley, H., Pinho, R. Simplified pushover-based earthquake loss assessment (SP-BELA) Method for Masonry Buildings. International Journal of Architectural Heritage. (2008)
- [35] Rota, M., Penna, A., Magenes, G. A methodology for deriving analytical fragility curves for masonry buildings based on stochastic nonlinear analyses. Engineering Structures, pp. 1312-1323 (2010)
- [36] Ceroni, F., Pecce, M., Sica, S., Garofano, A. Assessment of seismic vulnerability of a historical masonry buildings. (2012)
- [37] Abo-El-Ezz, A., Nolle, M., Naste, M. Seismic fragility assessment of low-rise stone masonry buildings. Earthquake engineering and engineering vibration, pp 87-97 (2013)
- [38] Frankie, T. K., Gencturk, B., Elnashai, A. S. Simulation-Based fragility relationships for unreinforced masonry buildings. Journal of structural engineering, pp 400-410 (2013)
- [39] Asteris, P. G., Chronopoulos, M. P., Chrysostomou. Seismic vulnerability assessment of historical masonry structural systems. Engineering structures, pp 118-134 (2014)

- [40] Simoes, A., Milosevic, J., Meireles, H., R., B., Cattari, S., Lagomarsino, S. Fragility curves for old masonry buildings types in Lisbon. *Bull Earthquake Eng*, pp. 3083-3105 (2015)
- [41] Furtado, A., Rodrigues, H., Arede, A., Varum, H. Simplified macro-model for infill masonry wall considering the out-of-plane behaviour. *Earthquake engineering and structural dynamics*, pp. 507-524 (2016)
- [42] Zuccaro, G., Dato, F., Cacace, F., De Gregorio, D., Sessa, S. Seismic collapse mechanisms analyses and masonry structures typologies: a possible correlation. *International Journal of Earthquake Engineering* (2017)
- [43] Rota, M., Penna, A., Magenes, G. A methodology for deriving analytical fragility curves for masonry buildings based on stochastic nonlinear analyses. *Engineering Structures*, pp 1312-1323 (2010)
- [44] Ferreira, T. M., Maio, R., Costa, A., Vicente, R. Seismic vulnerability assessment of stone masonry façade walls: calibration using fragility based results and observed damage. *Soil dynamics and earthquake engineering*, pp. 21-37 (2017)
- [45] Grunthal, G. European Macroseismic scale (1998)
- [46] Zuccaro, G. Progetto: SAVE - Strumenti Aggiornati per la Vulnerabilità Sismica del Patrimonio Edilizio e dei Sistemi Urbani Programma quadro 2000-2002 (2015)
- [47] Cundall, P. A., Strack, O. D. L. "Discrete numerical model for granular assemblies" *Geotechnique* 2: No. I, pp47-65 (1979)